NM~~P-~~H-CS~~ydro~~ 3~~1~~.0: a C# Programming L~~l~~anguage and Windows System based Ecohydrological Model Derived from Noah-MP

Yong-He Liu[1], Zong-Liang Yang[2]

[1] School of Resources and Environment, Henan Polytechnic University, Jiaozuo, Henan, China

[2] Jackson School of Geoscience, University of Texas at Austin, Austin TX, USA

Correspondence: Yong-He Liu (yonghe_hpu@163.com)

Abstract. The community Noah with multi-parameterization options (Noah-MP) land surface model (LSM) is widely used in studies from uncoupled land surface hydrometeorology and ecohydrology to coupled weather and climate predictions. In this study, we developed ~~NMP-Hydro~~NMH-CS 3~~1~~.0, a hydrological model written in CSharp(C#). ~~NMP-Hydro~~NMH-CS 3.0 is a new model~~was~~ developed by faithfully translating the FORTRAN version Noah-MP from the uncoupled WRF-Hydro 3.0, and ~~was~~is coupled with a river routing model. ~~NMP-Hydro~~NMH-CS has the capacity of execution on Windows systems, utilizing the multi-core CPUs commonly available in today's personal computers. The code of ~~NMP-Hydro~~NMH-CS has been tested to ensure that it produces a high-degree of consistency with the output of the original WRF-Hydro. High-resolution (6 km) simulations were conducted and assessed over a grid domain covering the entire Yellow River Basin and the most ~~part~~ of North China. The spatial maps and temporal variations of many state variables simulated by ~~NMP-Hydro~~NMH-CS ~~1~~3.0 and WRF-Hydro/Noah-MP demonstrate highly consistent results, with occasionally minor discrepancies. The river discharge for the Yellow River simulated by the new model with~~under~~ various scheme combinations of six ~~Noah-MP~~ parameterizations ~~exhibits~~exhibit general agreement with the natural river discharge at the Lanzhou station. ~~NMP-Hydro~~NMH-CS can be regarded as a reliable replica of Noah-MP in WRF-Hydro 3.0, but it can leverage the modern, powerful, and user-friendly features brought by the C~~-~~# language to significantly improve the efficiency of the model users and developers.

~~1.~~1 Introduction.

Formatted: Numbered + Level: 1 + Numbering Style: 1, 2, 3, … + Start at: 1 + Alignment: Left + Aligned at: 0 cm + Indent at: 0.63 cm

In contemporary hydrological prediction and flood warning applications, the effectiveness of hydrological models hinges on their ability to delineate intricate energy and water processes on the land surface, surpassing the capabilities of traditional rainfall-runoff models. To address this demand, certain land surface models (LSMs) utilized by atmospheric science communities have been bolstered with hydrological simulation features, as observed in WRF-Hydro (Lin et al., 2018)~~(Lin et al., 2018)~~, or conventional rainfall-runoff models have been enriched with more comprehensive descriptions of land surface processes, exemplified by the VIC model (Liang et al., 1994)~~(Liang et al., 1994)~~. The Noah Land Surface Model with multi-parameterizations (Noah-MP) (Niu et al., 2011; Yang et al., 2011)~~(Niu et al., 2011; Yang et al., 2011)~~stands out as a robust tool for studying global water issues, serving as the foundation for models like WRF-Hydro, which incorporates Noah-MP (Gochis, 2020)~~(Gochis, 2020)~~. However, the code for Noah-MP and WRF-Hydro is written in FORTARN, a

Field Code Changed

Field Code Changed

Field Code Changed

Field Code Changed

'legacy' language, posing challenges for code analysis and editing, unlike more modern languages such as CSharp(C#)~~ or Java~~, because FORTRAN lacks the similar intelligent efficient programming tools that are now common for C#. This limitation makes it arduous for users unfamiliar with FORTRAN to efficiently comprehend and modify the code. Additionally, Noah-MP and WRF-Hydro necessitate a UNIX-like operating system, causing inconvenience for the users and developers relying on Windows systems. Therefore, there is a compelling need to code Noah-MP in a contemporary modern programming language, to gain a wider accessibility of the Noah-MP model.

We designed ~~NMP-Hydro~~NMH-CS ~~1~~3.0, a Noah-MP based ~~h~~Hydrological model ~~based on Noah-MP but~~ coded using the CSharp (C#) programming language. This model was crafted by creating a framework and accurately translating the original Noah-MP LSM code from WRF-Hydro 3.0 and coupling with a Muskingum method-based river routing model(Liu et al., 2023)~~(Liu et al., 2023)~~. C#, recognized for its modern and object-oriented approach, is widely used for software development across various platforms, particularly on the Windows operating system. According to the TIOBE Programming Community Index (https://www.tiobe.com/) for October 2024, C# ranks fifth among major programming languages with a user base of 5.6%, while Fortran ranks ninth with only 1.8% of users.

~~NMP-Hydro~~NMH-CS provide~~soffers~~ several advantages over the original WRF-Hydro/Noah-MP. Unlike the original version that requires compiling for each computer and primarily~~edominantly relies~~ depends on Unix-like systems, ~~NMP-Hydro~~NMH-CS ~~can~~ can seamlessly run on Windows systems that support~~ing~~ the Microsoft Dotnet Framework. The executable files, once compiled, can be easily packaged and distributed to other Windows ~~computers~~machines, ~~providing~~ offers greater convenience for users who are less familiar with Unix-like operations. ~~-~~The utilization of the C# language facilitates advanced software ~~programs~~tools for ~~code~~ visualizing~~ation~~ and ~~analy~~analyse the model's code~~sis~~, enhancing the ~~user~~ convenience for users to ~~code~~ read~~ing,~~ ~~and~~ modify and debug the code~~ication~~. This is appealing to the model developers who are proficient in C# language and the object-oriented programming. The design of ~~model~~NMH-CS~~'s design~~ aligns with the input datasets and ~~settings~~ configurations specified in the 'namelist' file, ensuring high compatibility with WRF-Hydro 3.0. ~~Based on the support of~~Leveraging the parallel computing capabilities~~ation~~ of C#, both the translated Noah-MP LSM simulation and the river routing simulation within ~~NMP-Hydro~~NMH-CS support parallel execution on common personal computers.

2 The Noah-MP LSM

Noah-MP is a robust model renowned for its capability to represent diverse physical processes. Since its initial introduction~~ by~~ (Niu et al., 2011)~~Niu et al. (2011)~~ ~~and~~ (Yang et al., 2011)~~Yang et al. (2011)~~, Noah-MP has been widely used. For example, Noah-MP has been coupled to WRF-Hydro as a major module, and can be ~~has been~~ seamlessly integrated into the Weather Research and Forecasting (WRF) model~~, giving rise to the WRF-Hydro model, as elucidated by~~ (Gochis, 2020)~~Gochis (2020)~~. Furthermore, the offline WRF-Hydro model plays a pivotal role in the National Water Model, contributing to the simulation of floods and river flows across the United States~~, as highlighted by~~ (Bales, 2019)~~Bales (2019),~~ (Francesca et al., 2020)~~Francesca et al. (2020), and~~ (Karki et al., 2021)~~Karki et al. (2021)~~. Noah-MP's versatility extends to applications such as streamflow prediction (Lin et al., 2018)~~(Lin et al., 2018)~~ and the estimation of ~~spatial distributions for~~ evapotranspiration, surface temperature, carbon fluxes, heat fluxes, and soil moisture, as demonstrated in many studies (Chang et al., 2020; Gao et al., 2015; Li et al.,

Field Code Changed

Formatted: Font: (Asian) +Body Asian (等线), (Asian) Chinese (Simplified, Mainland China)

Field Code Changed

Field Code Changed

Field Code Changed

Field Code Changed

Field Code Changed

Field Code Changed

Field Code Changed

Field Code Changed

2022; Ma et al., 2017; Yang et al., 2021)~~(Chang et al., 2020; Gao et al., 2015; Li et al., 2022; Ma et al., 2017; Yang et al., 2021)~~. ~~.~~Noah-MP is supported by several different modelling frameworks to facilitate coupling it to various earth system framework models including HRLDAS (Chen et al., 2007), LIS(Kumar et al., 2006), and WRF-Hydro(Gochis, 2020). This makes Noah-MP a powerful research and forecasting tool within the hydrology community.

Noah-MP excels in physical~~ly~~ represent~~ation~~ation of~~ing~~ water and energy dynamics across various environmental layers, ~~encompassing~~ including a vegetation canopy layer, multiple snow and soil layers, and an optional unconfined aquifer layer for groundwater. ~~Unlike functioning in isolation, Noah-MP is typically coupled with host models, such as the community WRF-Hydro modelling framework (Lin et al., 2018) and HRLDAS (Chen et al., 2007), emphasizing its collaborative nature. Additionally, Noah-MP plays a pivotal role in the National Water Model (Francesca et al., 2020; Gochis, 2020), contributing to real-time streamflow forecasts for the entire United States of America.~~ To capture specific physical processes, Noah-MP employs multiple parameterization schemes, ~~offering~~ providing users the flexibility to choose~~select~~ from a total of 12 parametrizations, as detailed~~outlined~~ in Table 1. This versatility enables tailored representation of diverse environmental conditions and processes, enhancing the model's adaptability and applicability.

Formatted: No widow/orphan control

Table 1: Parameterization o~~O~~ptions for Noah-MP (an asterisk (*) denotes the recommended default option). Certain abbreviations correspond to terms used for Parameterization Schemes (PS) in Noah-MP, and their meanings can be referenced in the ~~Noah-MP~~WRF-Hydro 3.0 user document (Gochis et. al., 2015). ~~For instance, LAI and FVEG represent the leaf area index and the fraction of vegetation cover, respectively.~~ Note that these options may not be applicable to other versions of Noah-MP, such as that used in HRLDAS. The scheme options here are presented by some abbreviation marks such as ‘Noah’ or Schaake96 are those used in the ‘namelist’ file for Noah-MP.

Abbreviation	Physical parameterization	Scheme Code	Scheme Options
DVEG	Vegetation option	1~5	*1 table LAI, read FVEG; 2 dynamic LAI, FVEG=f(LAI); 3 table LAI, FVEG=f(LAI); 4 table LAI, FVEG=maximum; 5 dynamic LAI, FVEG =maximum
CRS	Stomatal conductance (controls transpiration from leaves)	1~2	*1 Ball-Berry; 2 Jarvis
BTR	β-factor (soil moisture stress factor controlling transpiration)	1~3	*1 Noah; 2 CLM; 3 SSiB
RUN	Runoff (runoff generation at and below the surface)	1~4	1 SIMGM; 2 SIMTOP; *3 Schaake96; 4 BATS
SFC	Surface layer drag coefficient	1~2	*1 M-O; 2 Chen97
FRZ	Frozen soil permeability	Fixed to 2	*1 NY06; 2 Koren99
INF	Supercooled liquid water	Fixed to 2	*1 NY06; 2 Koren99
RAD	Radiation transfer option	1~3	1 gap=F(3D,cosz); 2 gap=0; *3 gap=1-Fveg

ALB	Snow surface albedo	Fixed to 2	1 BATS; *2 CLASS
SNF	Precipitation partition option (rainfall or snowfall)	Fixed to 2	*1 Jordan91; 2 BATS; 3 Noah
TBOT	Lower boundary of soil temperature	1~2	*1 zero-flux; 2 Noah
STC	Snow/soil temperature time scheme	Fixed to 1	*1 semi-implicit; 2 fully implicit; 3 Ts=f(fsno)

3 Development of NMP-HydroNMH-CS

3.1 Translation of Noah-MP Code

Our primary focus in developing NMP-HydroNMH-CS involvesd translating the original FORTRAN code of Noah-MP into the C# language. The overarching objective of this translation is to create a hydrological model based on Noah-MP capable of functioning seamlessly on Windows systems. It is essential to note that this translation is based on a relatively older version of Noah-MP utilized in WRF-Hydro 3.0, as the process was startedcommenced before the release of Noah-MP 5.0 (He et al., 2023)(He et al., 2023).

Converting FORTRAN code into C# is not straightforward due to significant syntax differences in syntax between the two languages. The reconstruction of the model in the C# language follows an straightforward object-oriented design. While FORTRAN is traditionally a function-based language, the core Noah-MP module's functions, subroutines, and state variables are encapsulated as members within a C# class named GridCell (**Fig. 1(a)**). This class represents all Noah-MP behaviors within a grid box. The variable names, function definitions, data structures, and execution logic have been kept largely consistent with the original FORTRAN code, ensuring user-friendliness for those familiar with Noah-MP. To handle the execution on multiple grid boxes, another C# class named Driver is employed. This class manages tasks such as initializing model variables, creating multiple grid boxes, reading/writing files, and controlling the execution of the model.

Throughout the translation process, a key focus was addressing operations on FORTRAN arrays (**Fig. 1(b)**), crucial for representing the state of soil and snow layers in Noah-MP. Unlike C#, FORTRAN allows arrays to have user-specified index ranges (e.g., index values from -3 to 4). However, in C#, the first index of all arrays invariably starts from 0. To streamline the translation, we introduced designed a newwrapping array class of C# arrays, named FortArray,, designed to mimic FORTRAN arrays. The wrapped inner array data in FortArray adheres to standard C# conventions, accepting 0 as the inner index of the first element. Yet, externally, the class allow access to the array values through extra indices. by The class providinges methods for index translation from outer indices (FORTRAN style) to inner indices (C# style):

$$I_{in} = I_{ex} - I_{start} \quad (1)$$

Where I_{in}, I_{ex} and I_{start} represent the inner index, the outer index and the first outer index. The inner index corresponds to the standard C# arrays, while the outer index corresponds to the FORTRAN arrays. For instance, if a FORTRAN array of 8 elements has an index range from -3 to 4, this arrayit will be is translated into a FortArray that has a standard inner array of 8 elements, and accompanied by two

Field Code Changed

arguments representing the starting FORTRAN index (-3) and the ending FORTRAN index (4), but ~~then~~ the range of its inner indices ~~are~~remain 0~7. This array translation technique ensures that all the original execution logic in Noah-MP is seamlessly preserved in ~~NMP-Hydro~~NMH-CS.

The model also supports parallel execution, implemented through the native parallel functionality of the C# language. The technique can~~se functions~~ efficiently allocate computational tasks ~~for distinct~~over the grid boxes to different ~~CPU~~ threads which can be executed by separate CPU cores. For instance, if a ~~specific~~ grid domain requires the execution over~~of~~ 2400 grid boxes, and the tasks are assigned to 8 threads, each thread is responsible for ~~completing~~ the ~~tasks~~ calculations on~~of~~ approximately 300 grid boxes. It's crucial to note that if the number of specified threads exceeds the ~~actual~~ number of CPU cores, several~~multiple~~ threads should be ~~may end up~~ executed by~~ing on~~ the same~~a single~~ CPU core. Therefore, specifying more threads than the available CPU cores does not contribute to an overall improvement ~~in execution speed~~.

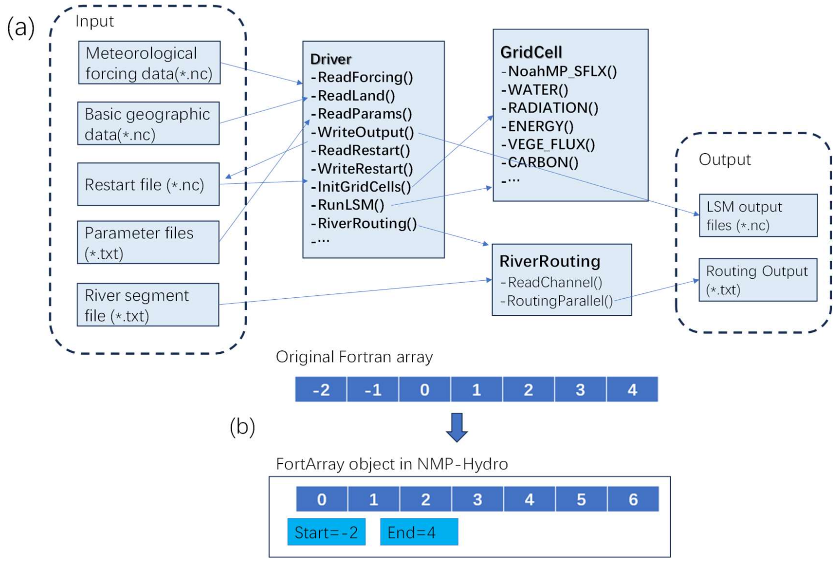

Figure 1. The architectural diagram of ~~NMP-Hydro~~NMH-CS (a) and the conversion of FORTRAN arrays to C# arrays (b). NMP-Hydro is a reconstructed replica of the version of Noah-MP that is coupled in WRF-Hydro 3.0.

Formatted: Font: 10 pt, Font color: Auto

3.2 ~~3.2~~ Coupling with a parallel river routing module

Formatted: Outline numbered + Level: 2 + Numbering Style: 1, 2, 3, … + Start at: 2 + Alignment: Left + Aligned at: 0 cm + Indent at: 0.63 cm

The Noah-MP land surface model can produce column outputs of runoff, but cannot simulate the horizontal movement of water. In order to simulating the surface movement of runoff in the river channels, we ~~In the development of NMP-Hydro, we~~ integrated a parallel river routing module, which is ~~-~~based on the Muskingum method for vectorized channel networks. ~~method~~The module is described in a previous study (Liu et al., 2023)~~;~~. This module is ~~deviating~~not ~~from~~ the previous ~~utilization of the coupled~~ RAPID model that was coupled in WRF-Hydro (Lin et al., 2018). This parallel river routing module, implemented using C#, incorporates our unique techniques.~~:~~

The first technique is a~~A~~n array-based sequential processing method for Muskingum routing. Muskingum-Cunge equation (Cunge, 1969) with lateral inflow considered is

$$Q_{e,t+1} = C_0 * Q_{s,t} + C_1 * Q_{s,t+1} + C_2 * Q_{e,t} + C_3 * Q_{lat,t+1} \quad (2)$$

Where

$$C_0 = \frac{kx + .5\Delta t}{k(1-x)+0.5\Delta t},\ C_1 = \frac{-kx+0.5\Delta t}{k(1-x)+0.5\Delta t},\ C_2 = 1 - C_0 - C_1,\ C_3 = \frac{\Delta t}{k(1-x)+0.5\Delta t}.$$

Here, Q represents the channel streamflow (m^3/s), which can be considered as a function of time and position. s is the start point of a channel segment/node, e denotes the end point of the channel segment, both of them are used as subscriptions for different spatial positions. n denotes the start of the period or inflow, $n+1$ denotes the end of the period or outflow. Both n and $n+1$ are used as subscriptions for position. The subscription 'lat' represents the lateral streamflow(runoff) from current river catchment.

Two parameters of the Muskingum-Cunge method are k and x. k is the travel time of a flow wave with celerity c_k through a channel segment of length L, thus $k=L/c_k$. Parameter x can be estimated by

$$x = \frac{1}{2}\left(1 - \frac{q}{S_o c_k L}\right) \quad (3)$$

Where q represents unit width streamflow, S_o is the channel bed slope.

The lateral inflow of each river segment is the runoff simulated by column Noah-MP LSM in NMH-CS, which is expressed as

$$Q_{lat,t} = R_{c,t} A_s \quad (4)$$

Where $Q_{lat,t}$ is the lateral inflow at time t, R_c is the runoff value at the given grid box, A_s is the local catchment area of current channel segment.

The form of Eq.(2) implies that the river routing calculation can be completed from any upstream river segment to its downstream segment. At the time $t+1$, all the outflows ($Q_{e,t+1}$) of multiple upstream segments will be summed up as the inflow ($Q_{s,t+1}$) of current segment. Although a common river network is a tree-like structure, it can be represented as a sequential array, where any upstream river segment is stored near the array head (with zero index), while its downstream river segment is stored near the array's tail (with large array index). Therefore, the Muskingum routing can be calculated over the river segment array in a unidirectional processing way (please see Fig.1 in Liu et al. (2023)).

~~(1)~~ The second technique is the ~~A~~ straightforward equal-sized domain decomposition method to conduct parallel calculation: just allocating the river segments into equal-sized blocks. Within each block, the Muskingum routing can be executed separately by a single CPU core. This treatment is based on that in any block, most segments have upstream segments within the same block, and only a small fraction of the segments have upstream segments in other blocks. Therefore, all river segments that receive inflows from other blocks (referred to as 'cross-block segments') need to be identified. These cross-block segments should be executed by the primary core, after the multi-domain parallel execution is completed.

~~(2)~~

~~(3)~~ The third technique is a~~Three distinct parallelization schemes for river routing.~~

~~4) A~~ specific sorting approach for river segments used in domain decomposition. It has been proven that a depth-first traverse of the river segments is more suitable for the parallel execution of the Muskingum method, compared to a width-first traverse, due to less cross-block segments in the blocks.

Formatted: No widow/orphan control
Formatted: Font: 10 pt
Formatted ... [1]
Formatted ... [2]
Formatted ... [3]
Formatted ... [4]
Formatted: Font: 10 pt
Formatted: Indent: First line: 0 cm
Formatted: Font: 10 pt
Formatted: Indent: First line: 0 cm
Formatted ... [5]
Formatted ... [6]
Formatted: Font: 10 pt
Formatted: Normal, No bullets or numbering
Formatted ... [7]
Formatted: Normal, No bullets or numbering
Formatted: Indent: Left: 0 cm, First line: 0 cm
Formatted ... [8]

This module requires two additional inputs files, a river segment list file named 'ChannelOrder.txt' and a 'namelist.txt' file. The latter file is used to set parameters and the length of time step. Each river segment in the list file presents following information: its own index, the index of its next downstream river segment, the row number and the column number of the grid box (in Noah-MP's running domain) providing runoff input to the current segment, the length (m) of the current river segment, the two parameter values (*K* and *X*) of the Muskingum method, the area of the catchment of the current segment.

The river segment list can be derived from both gridded river network or vectorized river network. The resolution of the river routing is determined by the original river network from which river segments is derived. Therefore, the choice of using vector river network or gridded river network and the selection of spatial resolution are completely determined by the users. The length of the temporal step of the river routing is required to be multiple times shorter than the time step for running the Noah-MP, and can also be designated by the users. For example, the time step of routing is set to 600s, while the time step for Noah-MP LSM is usually set to 3 hours.

This approach's primary advantage lies in its ability to ~~straightforwardly~~ simply decompose any river network into multiple domains with an equal number of river segments. Achieved by evenly dividing the river segment list into any number of blocks, this innovation capitalizes on the inherent tree-like structure present in most river networks. Importantly, it does not necessitate consideration of the topological conditions specific to a given network, as required in studies such as Mizukami et al. (2021) or David et al. (2015). This design allows parallel execution of river routing on modern personal computers equipped with multi-CPU cores.

The integration of the river routing module with the Noah-MP LSM involves assigning lateral inflows from the LSM-simulated total runoff to the river routing model. In the present ~~NMP-Hydro~~NMH-CS configuration, we utilize a ~~straightforward~~ catchment centroid-based coupling interface (David et al., 2015). This method designates the LSM grid cell containing the catchment centroid (referred to as the "centroid cell") as the location for a river reach to receive lateral inflows. At a specific temporal step, the computed contributing runoff discharge Q_{lat} (unit: m^3/s) is determined by the following expression:

$$Q_{lat} = R(nx, ny) \times F \times 1000 \qquad (5)$$

where $R(nx, ny)$ is the runoff (mm, surface + subsurface) simulated by the LSM during the time step, F is the catchment area (km^2) contributing water to the current river segment.

Alternatively, employing weighted assignments from different grid boxes, akin to the method utilized in (Lin et al., 2018), is also a valid approach. However, this method requires the generation of weights from multiple grid boxes. Given the rough resolution of the meteorological datasets~~size of each grid box (equivalent to the resolution of meteorological data, typically ranging from 25 km to 100 km)~~, ~~and considering that~~ each grid box can encompass the catchment areas of multiple river segments, the coupling approach using area weighting is unlikely to yield substantial improvements for most river segments.

Formatted: Indent: Left: 0 cm
Formatted: Font: Italic
Formatted: Font: Italic
Formatted: Indent: Left: 0 cm
Formatted: Indent: First line: 0 cm

3.3 Code Debugging Process

To eliminate any potential code errors resulting from incorrect translation, we conducted a thorough checkingreview of the code by performing model execution benchmark tests on single-column running on specific grid boxesa grid domain. Here, In the large domain (the same domain described in section 4.1), each time the grid box for single-column execution is arbitrarily selected. Such debuggingThese tests were carried out in twothree approaches stages. The first approach was Initially, the code underwentcarrying out a meticulous step-by-step checkdebugging by examining the printed values of manyeach variables (including many local variables in the code) in WRF-Hydro 3.0 running for specific single grid boxes. –This debugging process was also conducted repeated by switchingon each option of multiple physical parameterization schemes. The grid box for the single-column debugging was also switched several times. Such debuggingThis process has been conducted numerous times and has effectively eliminated any code errors arising from inaccurate translation. Although meteorological driving data for the debugging simulation is prepared for the period between 2000 and 2016, However, it is important to note that such debugging these tests are only feasible for a limited number of temporal steps– andfor a –grid- box execution. It is also impossible to conduct debugging on the entire domaines. The second approach is an artificial code checking process. Considering that the stepwise Ddebugging the code through years-long simulations across the entire domain is impractical, we checked the NMH-CS's code by comparing with the original FORTRAN code for many times. Through this checking, many code inconsistences were identified and corrected. .

In the second phase, we compared the spatial distribution of multiple state variables and the long-term discharge hydrograph produced at the main river sections by NMP-Hydro with that produced by WRF-Hydro 3.0. After identifying and correcting any erroneous code, the final results indicated that the two models are capable of generating broadly identical outcomes.

4. Benchmark Testing of NMP-HydroNMH-CS

4.1 Application area and data

4.1.1 Application area

The Yellow River Basin in Northern China is used as a test area of NMP-HydroNMH-CS. The gridded domain, as illustrated in **Fig.22 and Fig. 33**, encompasses the entirety of the Yellow River Basin (YRB) and the most part of North China, comprisingnsisting of 350 columns and 170 rows, featuring with a resolution of 6 km in Lambert conformal conic projection coordinates. Geophysical information data essential for the domain, including digital elevation, land use and land cover, and green vegetation fraction, wereas extracted from the WRF/WPS 3.5 input database.

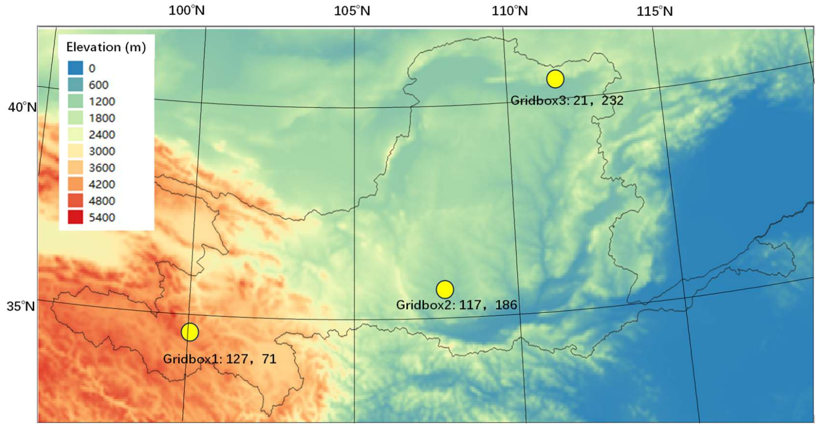

Figure 2. The terrain map of the simulation domain and the three grid boxes for comparison of state variable time series. The three grid boxes for extracting state variables to compare are represented by yellow dots, marked with grid box code, the row number and the column rows.

For the river routing simulation, the digital river network of the Yellow River was obtained from the HydroSHEDS dataset (version 1) (http://hydrosheds.cr.usgs.gov/). HydroSHEDS was~~is~~ derived from gridded digital elevation data with a resolution of 15 arc-seconds. Given the substantial human intervention and the intricate nature of reproducing observed daily or hourly water discharge, uniform values were assigned to all river segments for the river routing parameters (specifically, the wave celerity (c_k) and another parameter (x) describing the river channel condition, as detailed in ~~(~~David et al. (~~,~~ 2013~~)~~). No precise calibration is required here, as monthly or annual river discharge remains unaffected by changes in routing parameters.

The Yellow River basin experiences significant human impacts, including irrigation, industrial water usage, and groundwater extraction. Major artificial reservoirs and numerous smaller reservoirs regulate the river's discharge, serving as the primary water resource during the dry season. However, such extensive human interference presents substantial challenges in accurately modeling river discharge. Comparatively, the river discharge upstream of the Lanzhou (In Zone 1 as shown Fig.~~2~~3) hydrological station contributes over half of the entire YRB's total discharge, and is relatively less impacted by dams, enabling us to ~~objectively~~ test the model's performance.

Formatted: Font: (Default) Times New Roman, 10 pt

Formatted: Font: Italic

Formatted: Font: Italic, Subscript

Formatted: Font: Italic

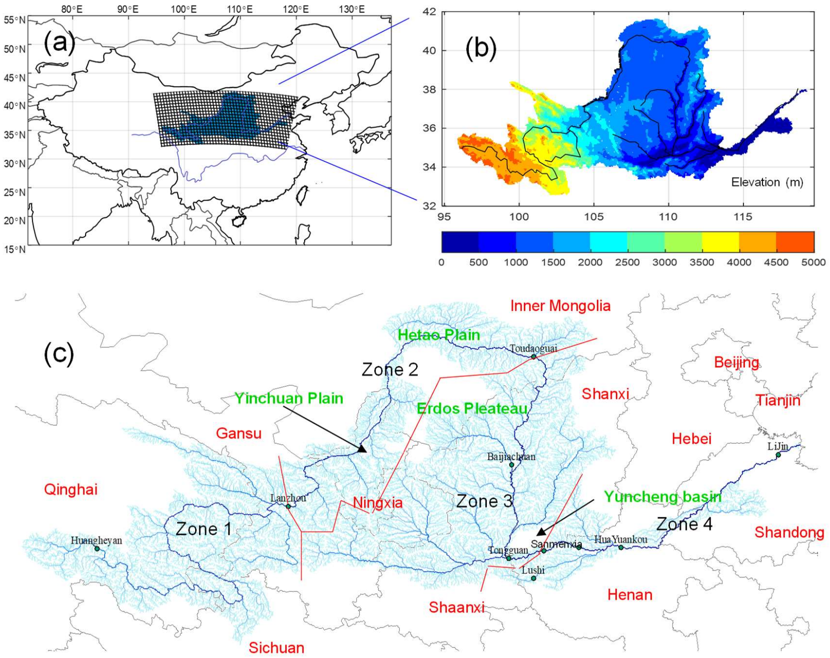

Figure 3. The grid domain covering the Yellow River Basin and the North China area: (a) Geographical location within China; (b) Elevations; (c) Vector River networks utilized for river routing modeling (extracted from the HydroSHEDS dataset). The delineation of the boundaries between distinct zones controlled by four gauging stations (Lanzhou, Toudaoguai, Sanmenxia, Lijin) is represented by red lines.

4.1.2 Meteorological dataset and river discharge data

To drive the two models (NMH-CS and WRF-Hydro), the same~~a~~ 3-hourly and 6-km grided meteorological forcing dataset comprised~~ing~~ of shortwave and longwave downward radiation, wind velocity, air temperature, relative humidity, air pressure at the surface, and precipitation rate was acquired. The benchmark dataset was ~~extracted~~clipped and regrided (bilinear interpolation) ~~–~~from the 1.0˚×1.0˚ GLDAS-1 land surface product (Gan et al., 2019; Rodell et al., 2004)~~(Gan et al., 2019; Rodell et al., 2004)~~, for the period 2000-2016. Given the limited availability of observational~~/reconstructed~~ river discharge data between 2001 and 2016, the extracted data pertains to this period, and additional data between 1996 and 2000 was also extracted for the model's spinning-up.

In previous research, the spinning-up of Noah-MP requires 50 years (Wu et al., 2021)~~(Wu et al., 2021)~~ or more than one hundred years (Zheng et al., 2019)~~(Zheng et al., 2019)~~ to achieve an equilibrium state. However, in this study, the spin-up process was conducted in two steps. In the first step, the period from 1996 to 2016 was run three times to generate a 'restart file' for a 63-year spinning-up, utilizing the initial PS combination~~ (11131-2222-121)~~. In the second step, starting from this initial combination, new schemes were ~~introduced~~adopted, and the 'restart file' obtained from the initial scheme combination was used to initiate the formal experiments covering the period from 1996 to 2016.

Field Code Changed

Field Code Changed

Field Code Changed

The dataset of Natural River Discharge (RND) reconstructed by the Yellow River Conservancy Commission of the Ministry of Water Resources was gathered to assess the model output. Annual natural discharges from the monitoring station of Lanzhou were collected for the period from 2001 to 2016.

4.2 Running speed

Compared to other differences between the two models, running speed is the least important factor to consider. Considering that NMH-CS and WRF-Hydro run on different platforms (Windows or Linux) and machines, it is also difficult to achieve a comparative evaluation of running speed. Actually, the comparison of running speed depends on the programming language used. In theory, FORTRAN and C programs can run faster than C# programs because FORTRAN and C are relatively low-level languages compared to any modern object-oriented language. However, as a language that can run in native machine code, C# is not slow. This means that there won't be a large difference in running speed between C# and FORTRAN. There are few authoritative publications on the running speed of these two languages, but there have been many documents on benchmark testing on the internet. When considering parallel execution, comparing the running speed of the two models also become more unnecessary. NMH-CS can run in parallel mode on personal computers, while WRF-Hydro does not have this functionality. On the other hand, WRF-Hydro can run in parallel mode in the Message Passing Interface (MPI) environment of high-performance computers, while NMH-CS does not support MPI.

We tested the execution time of NMH-CS by setting different numbers of C# parallel threads. The computer used for the testing is a common laptop with 6 CPU cores. The results indicate that for the execution of the entire domain, as the number of threads increases from 1 to 6, the average time consumed per time step is 1576ms, 977ms, 801ms, 711ms, 679ms, and 672ms, respectively. When the number of threads is set to 1, the time spent is slightly greater than the execution time in the non-parallel mode (1461ms). It is worth noting that the time spent is not linearly related to the number of parallel threads, which can be explained by various reasons. One is that some tasks are not actually executed in parallel mode, such as reading meteorological input files. Another reason is that not all threads in NMH-CS are fully processed by the CPU cores, as there are many other tasks in the entire Windows environment that have to be processed simultaneously by the CPU cores.

4.~~2~~3 Comparing the outputs of ~~NMP-Hydro~~NMH-CS and WRF-Hydro~~3.0~~

It is noteworthy that there are numerous parameterization scheme combinations for Noah-MP, which makes it unfeasible to compare the results generated under all scheme combinations. Therefore, the output of ~~NMP-Hydro~~NMH-CS and WRF-Hydro was compared only with ~~under~~ the default parameterization scheme combination~~ was compared~~, based on the exact same meteorological dataset. The comparison was conducted in two ways. The first comparison is that of the spatial maps of multiple variables (Table 2) for a specific year or day. For each state variable, such as SFCRNOFF, the maps of state variables simulated by ~~NMP-Hydro~~NMH-CS and WRF-Hydro are presented. The difference (Δ) between the values of the same variables simulated by the two 'Noah-MP models' is calculated as

$$\Delta = V_{\text{NMP-HydroNMH-CS}} - V_{\text{WRF-Hydro}} \quad (6)$$

Where $V_{\text{NMP-HydroNMH-CS}}$ and $V_{\text{WRF-Hydro}}$ are the state variable simulated by the two Noah-MP models, respectively.

Formatted: Font: (Asian) Times New Roman, 10 pt, English (United Kingdom)

Formatted: Font color: Red

Formatted: Font: (Asian) +Body Asian (等线), (Asian) Chinese (Simplified, Mainland China)

For certain variables, such as SFCRNOFF, UGDRNOFF, ECAN and ETRAN, the percent~~ive~~ relative differences were also calculated as follows:

$$\delta = 100 \cdot \Delta / V_{\text{WRF-Hydro}} \qquad (7)$$

The second method is to compare the temporal variations of state variables at specific grid boxes. In this case, only three grid boxes (Fig. 2) were selected to extract the state variable time series. The selection of these grid points is an arbitrary decision made by roughly considering different climate zones, without other strict consideration. Gridbox1 is selected from the Qinghai Plateau region, corresponding to the source region of the Yellow River. Gridbox2 corresponds to a location of Inner Mongolia and the north of Loess Plateau. Gridbox3 is in a hilly area of the Wei River Basin (a major part of the Yellow River Basin). In fact, during this study, other grid points also have been casually tested, but the results are mostly similar to the above mentioned 3 grid boxes. and will not be presented in the paper.

Table 2 The state variables simulated by ~~NMP-Hydro~~NMH-CS and WRF-Hydro, which is verified by generating maps

Variable name	description	unit
SFCRNOFF	Accumulated Surface runoff	mm
UGDRNOFF	Accumulated ground runoff	mm
ECAN	Evaporation from canopy	mm
ETRAN	Vegetation transpiration	mm
TV	Vegetation temperature	K
TG	Ground temperature	K
SOILT	The temperature for soil layers	K
SOILW (or SH2O)	The volumetric content of moisture in soil layers	$m^3 \cdot m^{-3}$
SNOWH	The total depth of snow layer	m
SNEQV	Snow water equivalent	$kg \cdot m^{-2}$
EAH	Canopy air vapor pressure	Pa
EVG	Ground evaporation heat	W·~~/~~m^{-2}
CHV	Exchange coefficient vegetated	m·~~/~~s^{-1}
CHLEAF	leaf exchange coefficient	--
TR	Transpiration heat	$W \cdot m^{-2}$~~W/m²~~
EVB	Evaporation heat to atmosphere bare	$W \cdot m^{-2}$~~W/m²~~
FIRA	Total net long-wave radiation to atmosphere	$W \cdot m^{-2}$~~W/m²~~
TRAD	Surface radiative temperature	K
ALBEDO	Surface albedo	--

4.3~~2~~.1 Maps of state variables ~~simulated~~

To test whether ~~NMP-Hydro~~NMH-CS can produce the corresponding outputs of the original WRF-Hydro (Fortran-version Noah-MP), many state variables (Table 2~~3~~) from multiple time slices ~~(10 June 2000, 10 June 2001, 10 June 2004, and 10 June 2008)~~ have been~~were~~ checked by drawing maps. ~~.~~ Only four slices (10 June 2000, 10 June 2001, 10 June 2004, and 10 June 2008) were arbitrarily selected here without special consideration. Only some maps of these state variables at certain time slices are presented in both the paper and the supplementary information. The maps for all the sate variables in Table 2 reflect

Formatted: Font: Italic
Formatted: Font: Italic
Formatted: Font: Italic
Formatted: Subscript
Formatted: Font: Not Bold
Formatted: Superscript
Formatted: Superscript
Formatted: Superscript

high consistence between NMH-CS and WRF-Hydro, with only ~~T~~the maps for two representative variables (SFCRNOFF and TV) are shown in **Fig.4 and Fig.**~~6~~**5**. As can be seen, there is visually little difference in the spatial patterns of the results. Similarly, no discernable visual difference is also apparent for the maps of other variables. However, the relative difference of annual surface runoff and annual underground runoff is significantly large at some areas (generally in high-elevation regions), where ~~NMP-Hydro~~NMH-CS underestimated those values ~~by~~ above 10%~~-30%~~ (**Fig.4**). For most of the domain~~Generally~~, the difference in TV is smaller than 0.2 ˚C, but in some sporadically districted locations, the TV's difference can be larger than 2 ˚C (**Fig.**5~~6~~). The comparison of TG has the similar effects, but the difference is more significant than that of TV. The similar high consistency effects are also reflected by other state variables, including soil temperature, soil water content, snow water equivalent (**Fig.S2-S4** in supplementary information). The differences in these state variables between the two models are generally small, except some large ones sporadically distributed in the high-latitude areas.

Formatted: Font: Bold

Formatted: Font: Bold

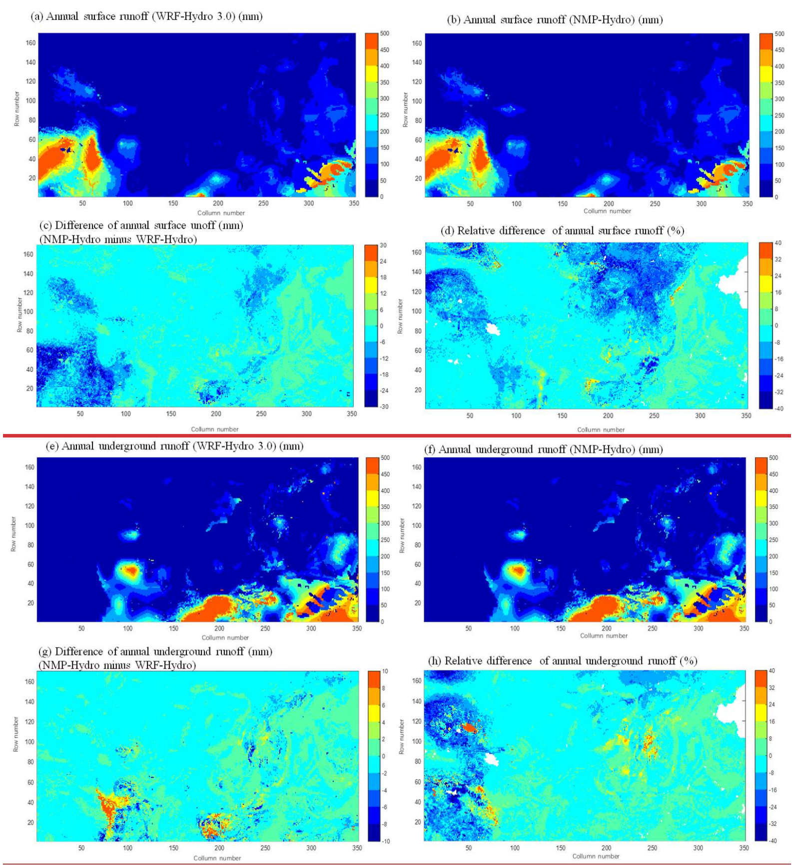

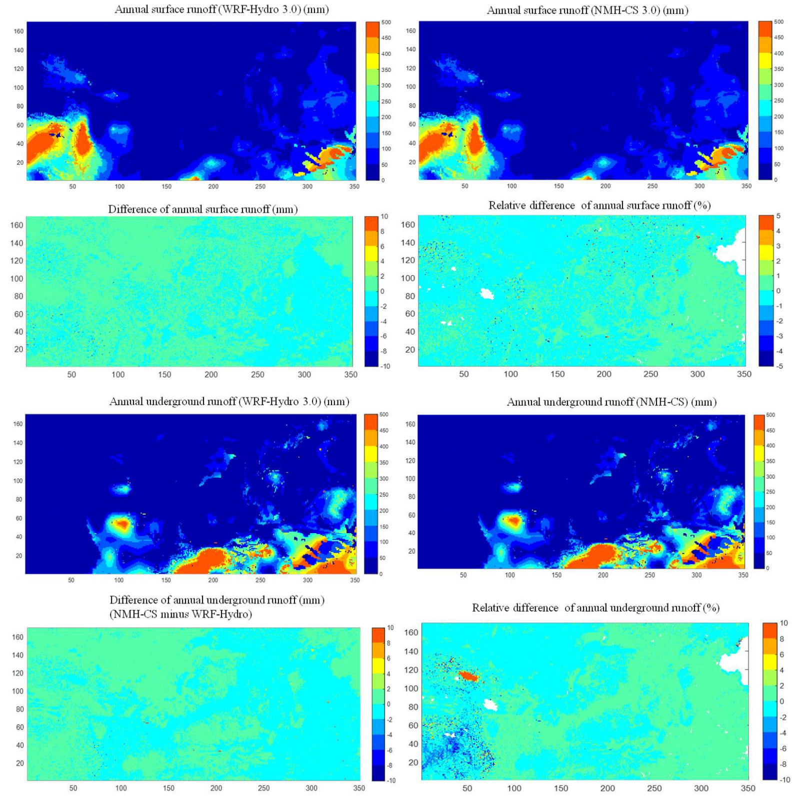

Figure 4. Maps of annual total values, differences, and relative differences of SFCRNOFF (surface runoff, mm) and UGDRNOFF (underground runoff, mm) simulated by WRF-Hydro3.0 and ~~NMP-Hydro~~NMH-CS ~~1~~3.0, for the year 2005.

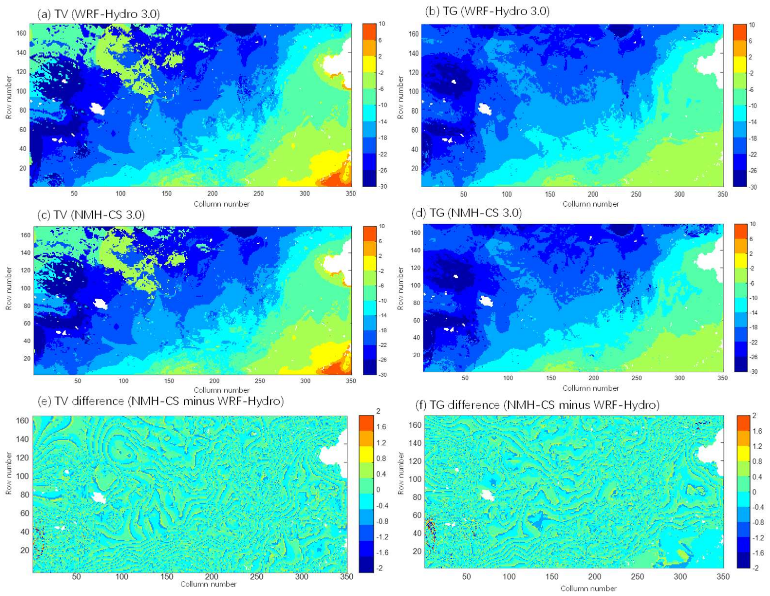

Figure 5: Maps of TV (vegetation temperature, ℃) and TG (ground temperature, ℃) simulated by WRF-Hydro3.0 and NMH-CS 3.0, for the day Jan. 1st, 2008.

4.3.2 Temporal variations of state variables

Formatted: Font: 小五

Formatted: Font: 小五

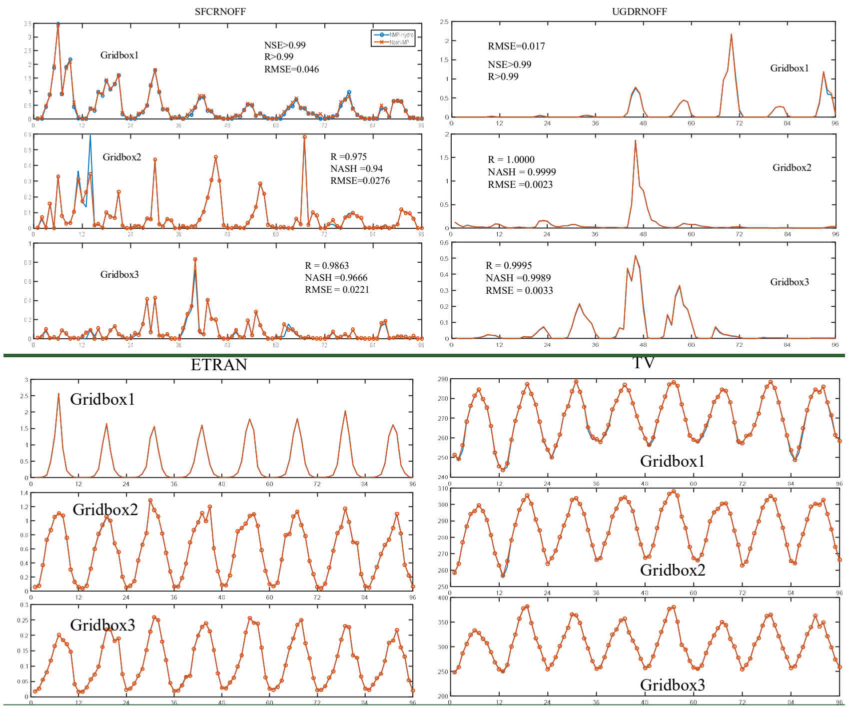

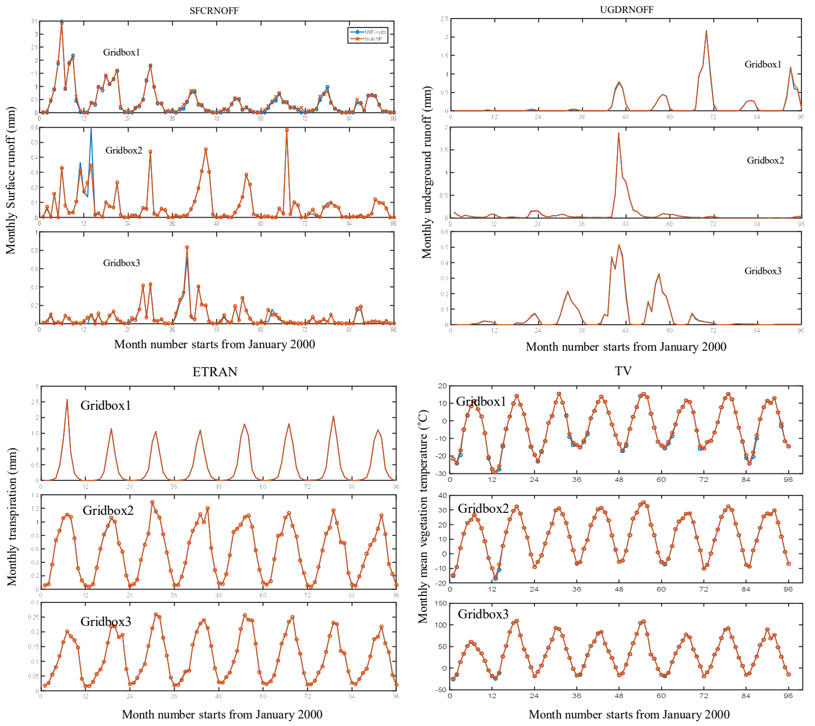

Figure 68: Monthly surface runoff (SFCRNOFF in mm), underground runoff(UGDRNOFF in mm), transpiration (ETRAN in mm) and vegetation temperature (TV in °C~~K~~) simulated by WRF-Hydro3.0(Noah-MP, blue) and ~~NMP-Hydro~~NMH-CS (red) at the three grid boxes, 2000-2007.

The ~~monthly temporal variations~~outputs at the~~of~~ three representative grid boxes (as shown in **Fig.2**) indicate that the two models produced consistent temporal changes (**Fig.~~8~~6, Fig.S5 and Fig.S6**). For certain variables, for example, SFCRNOFF~~、~~, TV and TG (other variables as well), ~~、FIRA、CHV,~~ occasionally, some significant differences were~~as~~ found in certain months for Gridbox2. It must be~~is~~ such occasionally happened differences that caused the spatial disparity as shown in **Fig.4-5**. We checked the disparity at certain grid boxes on the 3-hourly ~~daily scale~~values and found that the differences also happen sporadically (**Fig.57**). ~~Most of~~Almost all the disparities~~fferences~~ occur during the cold months (November, December, January, and February). However, it is worth noting that mostly ~~of~~ the simulated state variables ~~SFCRNOFF~~ in these months show no difference~~, and this difference is also independent of whether precipitation occurred during these days. Each difference is caused by a mismatch in the simulated peak time (Fig.5), manifested as a one day lag effect of NMP-Hydro relative to WRF-Hydro. Meanwhile, this lag effect of NMP-Hydro also causes underestimated or overestimated total surface runoff.~~ Considering such mismatch usually happens in cold months and high-elevation regions, it may be caused by the different calculation accuracy for the processes of ~~ice,~~ snow or~~and~~ frozen soil. For the three representative grid boxes, no significant differences were

Formatted: Font: (Default) +Body (等线), 五号

Formatted: Justified, Automatically adjust right indent when grid is defined, Adjust space between Latin and Asian text, Adjust space between Asian text and numbers

Formatted: Font: Bold, Font color: Red identified for certain variables, including many variables like TR, EAH, TV, ETRAN, UGDRNOFF (no plots for these variables will be presented in the paper).

By comparing and analyzing the printed state variables (in 3-hourly timesteps) in WRF-Hydro and the NMH-CS, we found the major inconsistencies occur in the module of snow water (named 'SNOWWATER' in the code). Although the code for these processes in Noah-MP is complex enough, we have checked the code multiple times and have not found any coding difference, so these differences are likely the result of floating-point errors.

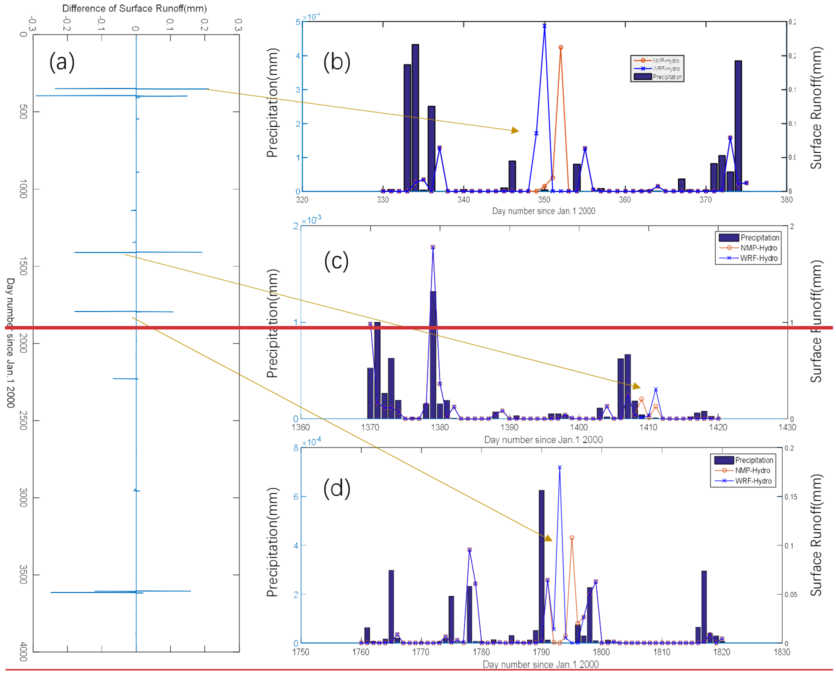

Figure 5. Simulated difference in daily surface runoff (SFCRNOFF) series simulated by NMP-Hydro and WRF-Hydro for Gridbox3. (a) the SFCRNOFF difference of NMP-Hydro to WRF-Hydro; (b-c) the disparities of SFCRNOFF near the day number 350, 1410 and 1790, respectively. From **Fig.7**, three major inconsistencies simulated between the two models occur usually simultaneously in the multiple state variables. These three cases demonstrates that almost all the major inconsistencies in multiple variables are caused by the minor inconsistencies in SNOWH (the state variable to indicate the depth of snow). The logic of snow process in Noah-MP is coded as when SNOWH is below 0.025m, the ISNOW (a state variable to indicate whether snow a layer exists) is set to zero (no snow layer), otherwise, is set to 1 (having a snow layer). Therefore, if SNOWH simulated by NMH-CS is close to 0.025, a small floating-point error may trigger a division between having a snow layer and no snow. Due to the different physical effects of radiation balance between snow layers and the ground, the distinction between having a snow layer and no snow layer will further lead to significant inconsistencies in snow depth (SNOWH), snow water equivalent (SNEQV), soil water (SOILW), vegetation temperature (TV), and ground temperature (TG). Once an inconsistency occurs, it will persist for a period of time. It is highly probable that the minor differences in SNOWH is caused by

Formatted: Justified

Formatted: Left, Automatically adjust right indent when grid is defined, Adjust space between Latin and Asian text, Adjust space between Asian text and numbers

Formatted: Font: Not Bold, Font color: Auto

Formatted: Font color: Auto

Formatted: Font: Not Bold, Font color: Auto

Formatted: Font: Not Bold

accumulation of floating-point error, because for most of the times the differences are very small except those during the inconsistent periods.

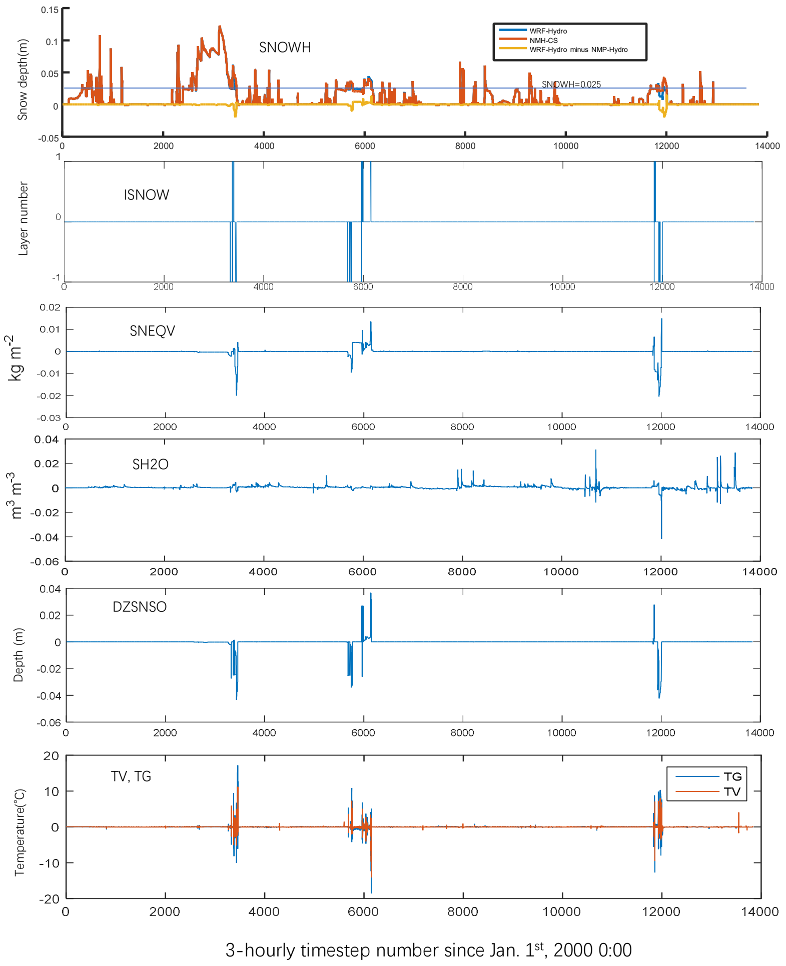

Figure 7: The differences (NMH-CS minus WRF-Hydro) between the three-hourly variables simulated by NMH-CS and those simulated by WRF-Hydro. SNOWH: snow depth (m); ISNOW: Number of snow layers, count; SNEQV: Snow water equivalent ($kg \cdot m^{-2}$); SH2O: soil liquid water content ($m^3 \cdot m^{-3}$), equivalent to SOILW; DZSNSO: snow/soil layer depth (m). These variable names are those used in the programming code. The occurring of the three inconsistencies correspond to the short periods: March 4, 2001, January 15, 2002 to February 8, 2002, and January 22, 2004 to February 9, 2004.

Given these discrepancies on a monthly scale, no NSE smaller than 0.9 and correlations smaller than 0.98 were identified. For the three representative grid boxes, no significant differences were identified for certain variables, including TR, EAH, TV, ACCETRAN, UGDRNOFF, and others (**Fig.8**). The daily

Formatted: Font: Bold
Formatted: Font: Bold
Formatted: Superscript
Formatted: Superscript
Formatted: Superscript

time series from multiple Gridbox3 grid boxes (including the three in Fig.2) wereare extracted, then andare compared between the NMP-HydroNMH-CS and the WRF-Hydro. Similar effects were obtained for the grid boxes, but only the results for Gridbox3 are presented as representative in **Fig.8**.– It is evident that EDIR, SFCRNOFF, soil water content (SOILW) and TV exhibit smallerr discrepancies, whereas TG and ALBEDO demonstrate largerr disparities (**Fig.7**). The discrepancies are pronounced when TG and TV below zero.The daily samples for soil temperature, soil water content, snow depth and snow water equivalent are presented in **Fig.S1, Fig.S5 and Fig.S6** (supplementary material). The comparisons about soil layers reflect that the soil temperature has relatively large inconsistencies, which should also be explained by the different division of snow layers that is caused by error when SNOWH approaches 0.025m.

Formatted: Font: Bold

Formatted: Font: Bold

The reason for occasional discrepancies between the outputs of two models remains elusive, as it is challenging to ascertain through the process of code checking and debugging. Such discrepancies may be attributed to a number of factors, including floating-point calculation errors, disparate parameter configurations, or encoding inconsistencies. The former two are reasonable and acceptable, whereas a coding mismatch is typically unacceptable. Nevertheless, identifying discrepancies is only feasible during the initial stages of debugging, but not for tens to hundreds of subsequent iterations. It is not uncommon for errors to remain undetected even after the execution of numerous time steps. In this study, in light of the fact that no inconsistencies remained after checking the code many times, it is plausible that floating-point errors play a significant role in explaining the discrepancies. During the debugging process, we found inconsistency always arise from the recursive calculation of energy transferring for vegetated and bare land, such as variables TV and TG. The floating-point error of temperature could potentially result in markedly divergent outcomes during transitions around frozen temperature.

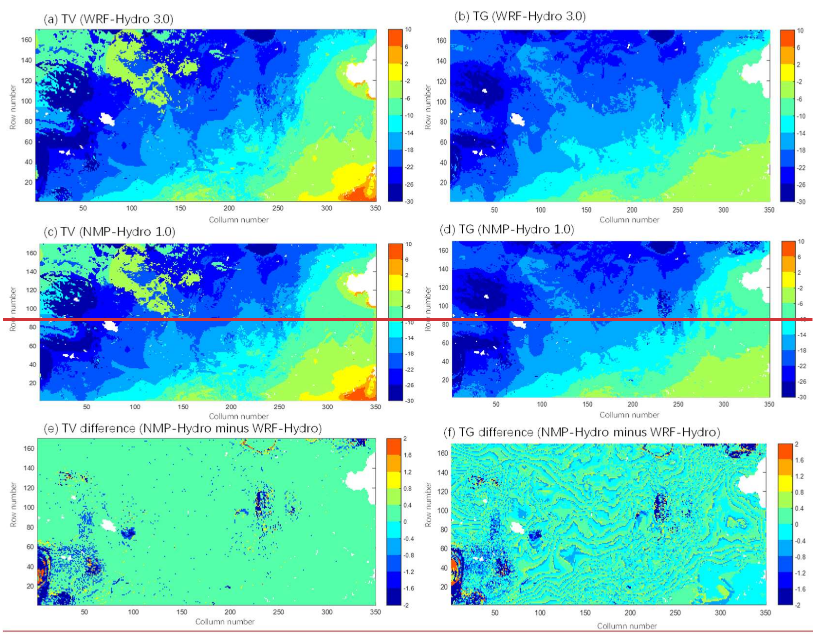

Figure 6: Maps of TV (vegetation temperature, K) and TG (ground temperature, °C) simulated by WRF-Hydro3.0 and NMP-Hydro 1.0, for the day Jan. 1st, 2008

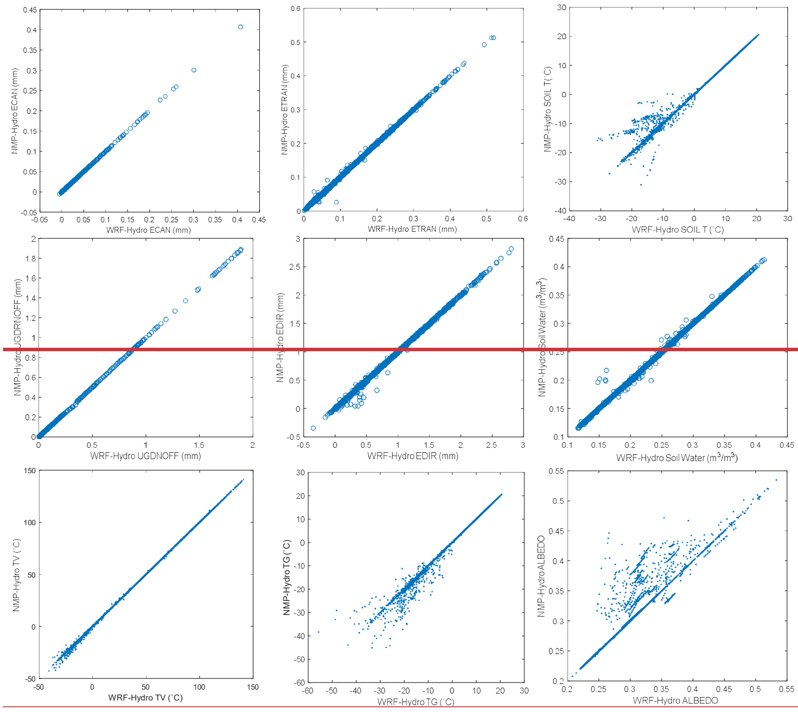

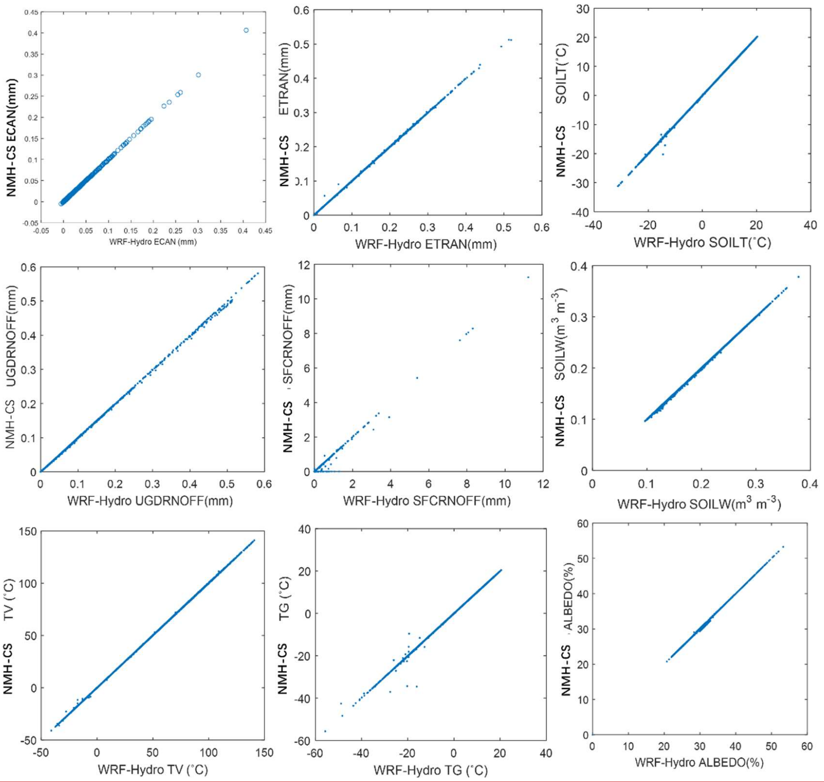

Figure 8~~7~~. Daily state variables simulated by ~~NMP-Hydro~~NMH-CS versus by WRF-Hydro at Gridbox3. Due to the high consistency for most of the values, statistical evaluation metrics such as correlation coefficients or relative biases will not be presented in the paper.

Formatted: Left

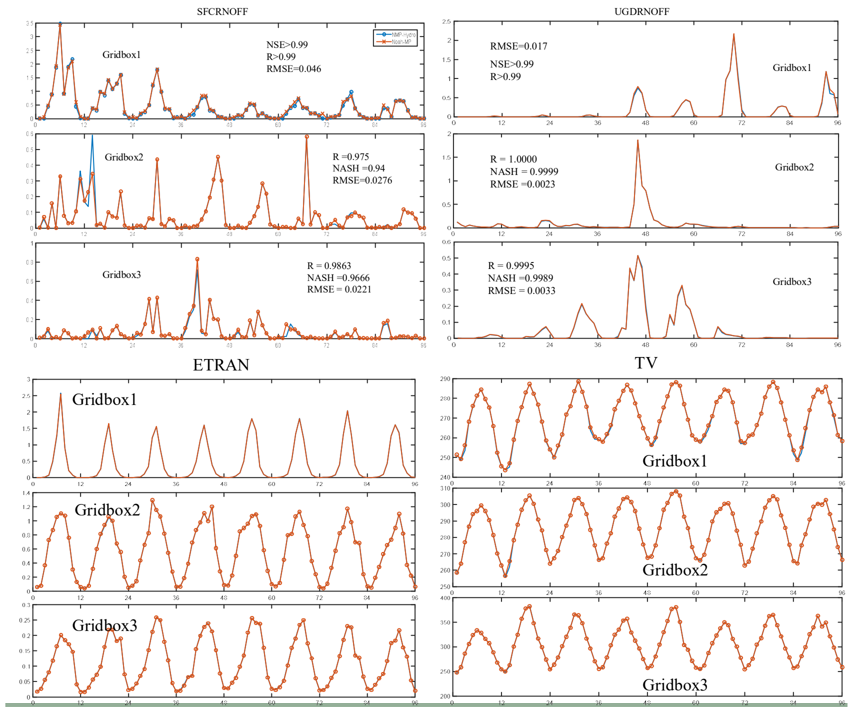

Figure 8: Monthly surface runoff (mm), underground runoff(mm), transpiration (mm) and vegetation temperature (K) simulated by WRF-Hydro3.0(Noah-MP, blue) and NMP-Hydro (red) at the three grid boxes, 2000-2007.

4.34 Streamflow discharges simulated by multiple experimentsfor the Yellow River by NMH-CS

4.34.1 Experimental design of Noah-MP simulation

Here, we present the numerical outputs of NMP-HydroNMH-CS and the comparison with WRF-Hydro/Noah-MP on the streamflow discharges over the Yellow River, with various parameterization schemes used. The parallel speedup of NMP-Hydro will not be evaluated here, as it is a straightforward implementation in C# for executing multiple tasks. The description of parallelization of the coupled river routing models has been clearly described in our previous publication(Liu et al., 2023).

To verify whether the various parameterization schemes (PSs) of NMP-HydroNMH-CS can produce reasonable discharge for the Yellow River catchment area, this study conducted 17 Noah-MP simulations using different PS combinations. Given the challenge of determining the relative importance of each parameterization and the impracticality of including all possible combinations, we adopted a strategic approach. A fixed PS combination was established as a foundation, and alterations were made to one parameterization's scheme at a time (refer to **Table 3**). In addition to our selected parameterizations, we considered commonly used PS combinations,

Formatted: Font: 五号
Formatted: Font: 五号
Formatted: Font: 五号, Bold
Formatted: Font: 五号

including the 'default' combination proposed by Noah-MP developers. Sensitivity analysis was conducted by analyzing the differences or variations among these incomplete PS combinations. It is important to note that the chosen PS combinations represent only a subset of all possible combinations, and the assumed sensitivities based on this subset are considered indicative of overall sensitivities based on the complete set of combinations.

The PS combinations are represented by codes consisting of sequential digital numbers. For instance, the default combination is denoted as '11131-1132-111', where each number signifies a scheme option. The initial experiment, arbitrarily set as the PS combination of '11131-2222-121', served as the foundation for subsequent experiments. Fifteen experiments (refer to Table 2) were then conducted by modifying one option at a time from the initial experiment.

These experiments are categorized into multiple groups, with the initial experiment '11131-2222-121' being employed in multiple groups:

Runoff scheme group (four experiments, switching between: 1. SIMGM, 2. SIMTOP, 3. Schaake96, 4. BATS);

Vegetation scheme group (five experiments, switching between the first option and the fifth option, see Table 1);

β-factor option group (three experiments, switching between Noah, CLM, and SSiB);

Radiation transfer option group (three experiments, switching between three options);

Group for the scheme of the lower boundary of soil temperature (six experiments);

Group for stomatal conductance scheme (two experiments, switching between two options).

Table 3. Experiments conducted in this study

Number	PS combination code	Abbreviated code	Description
1	11131-2222-121	11131 or 11131-222 or 11131*121	The control~~first~~ experiment
2	11111-2222-121	11111	Experiments with RUN
3	11121-2222-121	11121	
4	11141-2222-121	11141	
5	21131-2222-121	21131 or 21131*121	Experiments with DVEG
6	31131-2222-121	31131	
7	41131-2222-121	41131	
8	51131-2222-121	51131 or 51131*121	
9	11231-2222-121	11231	Experiments with BTR
10	11331-2222-121	11331	
11	11131-2212-121	11131-221	Experiments with RAD
12	11131-2232-121	11131-223	
13	12131-2222-121	12131	Experiments with CRS
14	11131-1132-111	‘default’	The default PS combination proposed by Noah-MP developers
15	11131-2222-111	11131*111	Experiments with TBOT

16	21131-2222-111	21131*111
17	51131-2222-111	51131*111

4.34.2 Simulated streamflow under various parameterization schemes

We simply use tThe Taylor diagrams (Taylor, 2001)(Taylor, 2001) are used to evaluate the different PS on the river discharge at the Lanzhou station. Taylor diagram provides a graphical representation of a model's simulation performance, encompassing three key indices: correlation coefficient (*R*), root-mean-square error (RMSE), and standard deviation (SD).

The streamflow discharges were produced by coupling the NMP-HydroNMH-CS with the parallel river routing model. The results showed that, in general, the various scheme combinations of parameterizations can produce monthly river discharge close to the result of the original Noah-MP (WRF-Hydro) for the Lanzhou station. A preliminary comparison on the various scheme combinations is presented in **Table 4**. The monthly performance is summarized in Table 4 based on the comparison of the different PSs as shown in **Fig. 9**. It can be observed that for the majority of parameterizations, the discharges in winter are not sensitive to the schemes, this is to be expected, given the minimal runoff during this season. The simulated summer discharges exhibit notable degree of sensitivity with regard to the various parametrization schemes. In relation to the runoff parametrization, the results obtained through the utilization of the SIGGM scheme led to overestimation during the winter season and underestimation during summer, signifying that considering groundwater could enhance the simulation accuracy of the catchment modulation as opposed to other schemes.

For the Lanzhou station, over 50% of experiments produced discharges with correlations larger than 0.9 (Fig.10). The PS combination '11141-2222-121' yielded the highest correlation, and '11131-2222-111' showed the highest performance according to Taylor's score.

Field Code Changed

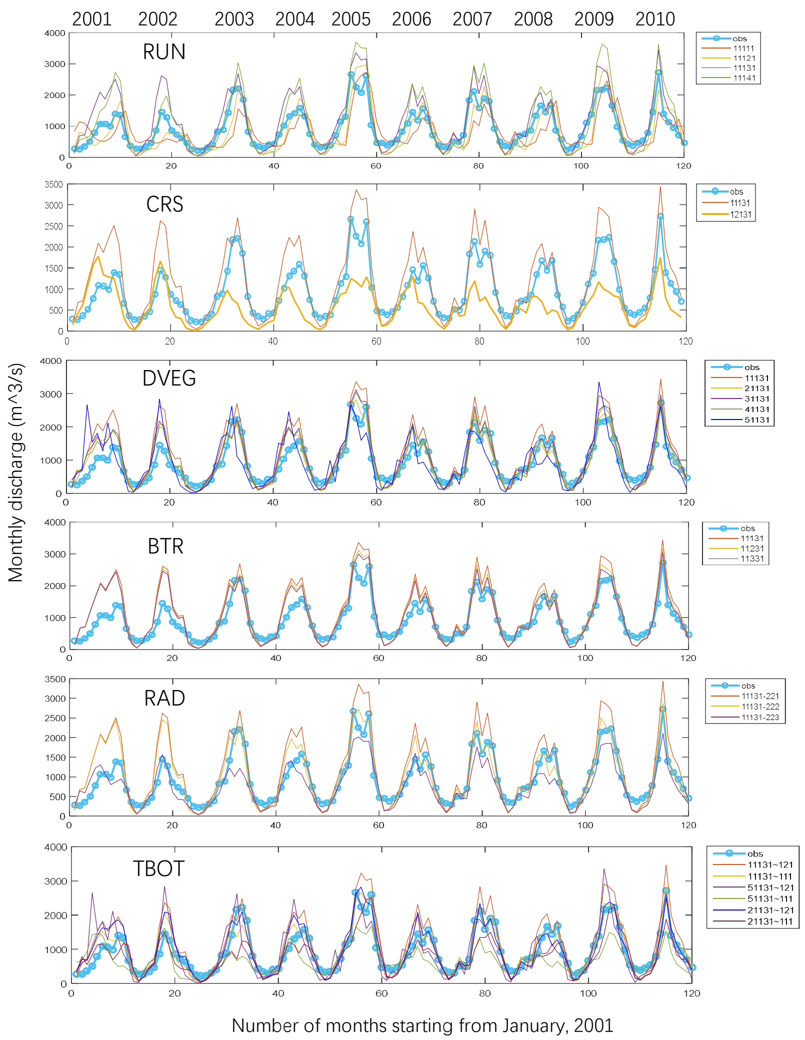

Figure 9: Simulated Mmonthly rRiver discharge (m^3/s) for Lanzhou by NMH-CS. The first subplot displays the results simulated with varying RUN schemes while the other subplots follow a similar pattern. Reconstructed natural discharge is denoted as 'obs'.

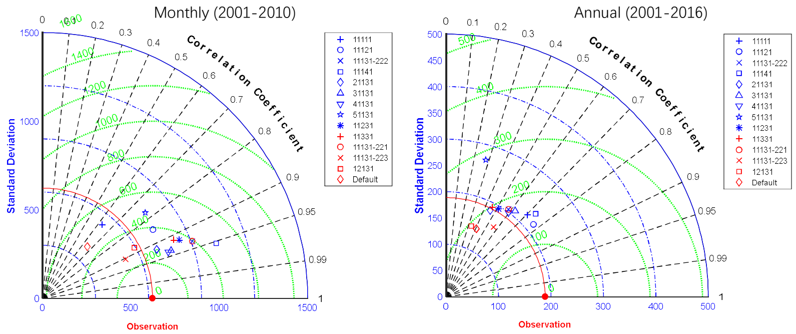

Figure 10: Taylor diagram for monthly and annual mean river discharge (m^3/s) at the Lanzhou monitoring station

Table 4: Performance of various parameterization schemes on monthly discharge for Lanzhou station

	scheme	Winter	summer
RUN	1.SIGGM	Overestimation	underestimation
	2.SIMTOP	underestimation	Small overestimation
	3.Schaake96		Large overestimation
	4.BATS		The Largest overestimation
CRS	1. Ball-Berry	Small difference	Overestimation
	2. Jarvis		Underestimation
DVEG	1.Table LAI, read FVEG	No significant difference	The largest overestimation
	2.dynamical LAI and FVEG=f(LAI)		Mostly small overestimation
	3. table LAI, FVEG=f(LAI)		
	4 table LAI, FVEG=maximum		
	5.Dynamical LAI, maximum FVEG	Unstable overestimation and underestimation	
BTR	1.Noah	No significant difference	The largest overestimation
	2.CLM		The middle overestimation
	3.SSib		The smallest overestimation
RAD	1. gap=F(3D, cosz)	No significant difference	Large overestimation
	2. gap=0		Slight overestimation
	3. gap=1-FVEG		underestimation
TBOT	1. Zero flux	No significant difference	large
	2.Noah		small

5 Discussions

5.1 Major advantages of NMH-CS

The original intention of developing a Noah-MP model with the C# programming language was to analyze and edit Noah-MP code in a more efficient way, as there are many modern and efficient tools

Formatted: Font: (Asian) Times New Roman, 10 pt, English (United Kingdom)

Formatted: Indent: First line: 0 ch

available for analyzing code written in C#, such as Microsoft Visual Studio, SharpDevelop (https://github.com/icsharpcode/SharpDevelop). There are almost no comparable powerful tools for analyzing FORTRAN code. This advantage is significant from the developers' perspective.

From the user's perspective, NMH-CS run on windows (although it should also run on other UNIX like platforms after some specific configuration in the future), which is more favorable for many Windows users around the world. On the windows system, in most cases, the NMH-CS software can be distributed at multiple computers by simply copying it, unlike that in Unix-like systems, compiling of the code is usually required.

5.3 Inconsistencies between the two models

As indicated by the previous analysis, the main inconsistency between the outputs of the two models (WRF-Hydro and NMH-CS) was found to be related to the transition between the presence or absence of snow layers. In Noah-MP, the existence of snow layers is determined by the depth of the snow (represented by the variable SNOWH in the code). When the SNOWH value approaches the threshold (0.025m), a small error will result in a division on the judgement whether a snow layer exists. This inconsistent division will further lead to significant differences in other state variables. However, this difference will not last long (as shown in Figure 3, up to 30-40 days). However, it is difficult to determine whether the errors in SNOWH are caused by the accumulation of floating-point errors or other errors.

There may be some other inconsistencies that has not been identified. Due to the complex nature of Noah-MP, it is challenging to identify all the minor differences through the process of code checking and debugging. Therefore, to ensure the results of two models to be completely consistent need a long-term process. Discrepancies can be arisen from multiple factors, including floating-point calculation errors, some inconsistent hardcoded parameter values (as local variables in certain modules), or inconsistent programming code. The former two are reasonable and acceptable, whereas a coding mismatch can cause unexpected outputs. From the scientific perspective, these minor differences between NMH-CS and WRF Hydro are not very critical, as the model users are always modifying the code during their research, and small changes in the code can lead to large different results. The existence of differences does not always mean that NMH-CS is inferior to Noah-MP in WRF-Hydro 3.0.

In most cases, identifying discrepancies is only feasible during the debugging of the first 1-3 timesteps, but not for tens to hundreds of subsequent iterations. It is not uncommon for errors to remain undetected even after the execution of numerous time steps. In this study, given that no code inconsistencies were found after multiple rounds of code checking, it is plausible that floating-point errors related to SNOWH (or other related variables) play a major role in explaining the remaining discrepancies.

Based on the debugging process, we also found that some variables such as TV and TG calculated by the two models always have slight inconsistencies, but they are almost insignificant on a daily or monthly scale. It is highly probable that such inconsistencies arise from the accumulated error caused by the recursive calculation of energy transferring for vegetated and bare land.

Formatted: Font: (Asian) +Body Asian (等线), English (United Kingdom)
Formatted: Font: (Asian) +Body Asian (等线), English (United Kingdom)
Formatted: English (United Kingdom)
Formatted: Heading 2, Space Before: 12 pt, After: 12 pt
Formatted: Left, Automatically adjust right indent when grid is defined, Adjust space between Latin and Asian text, Adjust space between Asian text and numbers
Formatted: Font: 10 pt
Formatted: Left, Indent: First line: 0 cm

65 Model code and technical documentation for NMP-HydroNMH-CS

We archive, manage, and maintain the NMP-HydroNMH-CS at https://github.com/lsucksis/NMP-HydroNMH-CS for public access. A technical description was provided at the same site. The original version of the model is also provided at the website of Science Data Bank: https://doi.org/10.57760/sciencedb.16102.

75 Conclusions

This study presents the NMP-HydroNMH-CS 31.0, which is a reconstructed land surface eco-hydrological model based on Noah-MP. –The model was developed by translating the FORTRAN code of Noah-MP (in WRF-Hydro 3.0) into C# and also coupling it with a river routing model. The model has been designed for parallel execution on Windows systems, thereby capitalizing on the multi-core CPUs that are now a standard feature of personal computers. The NMP-HydroNMH-CS code has been subjected to rigorous testing to ensure that it produces results that are as –consistent as possible with those of the original WRF-Hydro. The code is based on the C# language, which facilitates greater user-friendliness and facilitates modification and expansion.

The development of this software enabled the successful execution of high-resolution simulations encompassing a 6-km span within the Yellow River Basin (YRB). These simulations were conducted with a multitude of parameter scheme (PS) combinations within the Noah-MP framework. Maps of all the outputs (runoff, evaporation, groundwater, energy, vegetation) across the grid domain demonstrate consistent spatial patterns that are simulated by the two models. The long-term variations of multiple state variables simulated by the two models also exhibit high consistency, although some differences are evidentalso exist. Identifying the cause of this simulation discrepancy in the outputs of the two models is a challenging task, given the intricate nature of the Noah-MP code. The sporadic occurrence of errors may be attributed to the accumulation of floating-point numerical calculation errors, especially for the cases below frozen temperature.

With regard to the By enabling the coupled river routing model on river networkLanzhou hydrological station, the river discharge simulated by NMP-HydroNMH-CS 13.0 –based on the multiple scheme combination of parameterizations is found to be in reasonable agreement with the reconstructed natural river discharge, for the Lanzhou hydrological station.

The main inconsistencies in multiple variables between NMH-CS output and WRF-Hydro output was found to be related to inconsistent judgments on the presence of snow layers, which are caused by minor cumulative errors near the threshold value of 0.025m for snow depth. Overall, while there are occasionally happened disparities in the NMH-CS simulated results when compared to the original WRF-Hydro, it reproduces highly consistent spatiotemporal distribution of multiple variables as that by WRF-Hydro 3.0. It can therefore be asserted that NMH-CS can be considered a reliable replica of Noah-MP in the uncoupled WRF-Hydro 3.0.

Overall, while there are discrepancies in the simulated results when compared to the original model, the NMP-Hydro 1.0 reproduces consistent spatiotemporal distribution of multiple variables as that by WRF-Hydro 3.0. Given the complex nature of long-term state variables in Noah-MP, which reflect multiple processes including runoff production, energy transfer and dynamical vegetation, the results of NMP-Hydro and WRF-Hydro/Noah-MP remain highly consistent. It can therefore be asserted that NMP-Hydro can be considered a reliable replica of Noah-MP in the uncoupled WRF-Hydro 3.0. It was inevitable that

~~minor modifications to the code or model parameters would be required during the testing phase of NMP-Hydro. This presented a significant challenge in reproducing the identical outputs as those generated by WRF-Hydro.~~This new software NMH-CS can run on Windows system platforms. Its C# code can be analyzed and visually browsed using many modern intelligent tools such as those in Sharpdevelop or Microsoft Visual Studio. This feature makes the code easier to analyze and modify, which in turn will attract more users and promote the future development of the Noah-MP model. The current version of NMH-CS can serve as a good model for simulating land surface processes in climate change and ecohydrology research. Although NMH-CS cannot be used as a coupling module to other FORTRAN based framework models (such as the WRF model), it can still be used as a prototype system to improve the Noah-MP schemes. Any new improvements in NMH-CS can easily be updated to other FORTRAN based Noah-MP.

Future plans for the development of NMH-CS include (1) providing a single-column run mode and incorporating a genetic algorithm-based parameter optimization module; (2) extending the functionality for modelling dynamic vegetation by designing new schemes or optimizing parameters; (3) implementing major improved model physics that exists in later versions (for example the Noah-MP 5.0) of Noah-MP into the NMH-CS framework; (4) enabling the functionality of running on UNIX-like systems.

Formatted: Font: 10 pt
Formatted: Font: 10 pt
Formatted: Font: 10 pt
Formatted: Font: 10 pt

Acknowledgements. Thanks Pei-Rong Lin for her great efforts in guiding Yong-He Liu through the intricacies of Noah-MP.

Code and data availability. 1. The ~~NMP-Hydro~~NMH-CS model code is available at https://doi.org/10.57760/sciencedb.16102 ~~(Liu, 2024b)~~(Liu, 2024a). 2. The Noah-MP technical documentation is available at the same site and more details will continue to be added in the documentation. 3. The benchmark meteorological datasets for driving ~~NMP-Hydro~~NMH-CS and WRF-Hydro 3.0 were uploaded to the Science Data Bank (DOI: https://doi.org/10.57760/sciencedb.13122 (Liu, 2024b)~~(Liu, 2024a)~~).

Author contributions. Yong-He Liu has translated the code of WRF-Hydro/Noah-MP to ~~NMP-Hydro~~NMH-CS, the debugging and the benchmark model simulations. The work is led by Zong-Liang Yang. Liu has drafted the paper, with improvement made by Yang.

Competing interests. The contact author has declared that none of the authors has any competing interests.

Financial support. This work is funded by the Project on the Creation of "Double First-class" Disciplines in Surveying and Mapping Science and Technology (Grant No. GCCYJ202418), Henan Polytechnic University.

References

Bales, J.: Featured Collection Introduction: National Water Model II, J. Am. Water Resour. As., 55(4), 938-939, https://doi.org/10.1111/1752-1688.12786, 2019.

Biswa, K., Jamatia, B., Choudhury, D. and Borah, P.: Comparative Analysis of C , FORTRAN , C # and Java Programming Languages, ternational Journal of Computer Science and Information Technologies, 7(2), 1004-1007, 2016.

Chang, M., Liao, W., Wang, X., Zhang, Q., Chen, W., Wu, Z. and Hu, Z.: An optimal ensemble of the Noah-MP land surface model for simulating surface heat fluxes over a typical subtropical forest in South China, Agr. Forest Meteorol., 281, https://doi.org/10.1016/j.agrformet.2019.107815, 2020.

Chen, F., Manning, K.W., LeMone, M.A., Trier, S.B., Alfieri, J.G., Roberts, R., Tewari, M., Niyogi, D., Horst, T.W., Oncley, S.P., Basara, J.B. and Blanken, P.D.: Description and evaluation of the characteristics of the NCAR high-resolution land data assimilation system, J. Appl Meteorol Clim, 46(6), 694-713, https://doi.org/10.1175/JAM2463.1, 2007.

Cunge, J.A., 1969. On the subject of a flood propagation computation method (Muskingum method). Journal of Hydraulic Research.

Francesca, V., Kelly, M., Laura, R., Fernando, S., Bradford, B., Jason, E., Brian, C., Aubrey, D., David, G. and Robert, C.: A Multiscale, Hydrometeorological Forecast Evaluation of National Water Model Forecasts of the May 2018 Ellicott City, Maryland, Flood, J. Hydrometeorol., 21(3), 2020.

Gan, Y., Liang, X., Duan, Q., Chen, F., Li, J. and Zhang, Y.: Assessment and Reduction of the Physical Parameterization Uncertainty for Noah-MP Land Surface Model, Water Resour. Res., 55(7), 5518-5538, https://doi.org/10.1029/2019WR024814, 2019.

Gao, Y., Li, K., Chen, F., Jiang, Y. and Lu, C.: Assessing and improving Noah-MP land model simulations for the central Tibetan Plateau, J. Geophys. Res.-Atmos., 120(18), 9258-9278, https://doi.org/10.1002/2015JD023404, 2015.

Gochis, D.J., W. Yu, D.N. Yates, 2015: The WRF-Hydro model technical description and user's guide, version 3.0. NCAR Technical Document. 123 pages.

Gochis, D.J.A.C., 2020. The WRF-Hydro modeling system technical description (version 5.1.1). NCAR Tech. Note.

He, C., Valayamkunnath, P., Barlage, M., Chen, F., Gochis, D., Cabell, R., Schneider, T., Rasmussen, R., Niu, G.Y., Yang, Z.L., Niyogi, D. and Ek, M.: Modernizing the open-source community Noah with multi-parameterization options (Noah-MP) land surface model (version 5.0) with enhanced modularity, interoperability, and applicability, Geosci Model Dev, 16(17), 5131-5151, https://doi.org/10.5194/gmd-16-5131-2023, 2023.

Karki, R., Krienert, J.M., Hong, M. and Steward, D.R.: Evaluating Baseflow Simulation in the National Water Model: A Case Study in the Northern High Plains Region, USA, J. Am. Water Resour. As., 57(2), 267-280, https://doi.org/10.1111/1752-1688.12911, 2021.

Kumar, S.V., Peters-Lidard, C.D., Tian, Y., Houser, P.R., Geiger, J., Olden, S., Lighty, L., Eastman, J.L., Doty, B., Dirmeyer, P., Adams, J., Mitchell, K., Wood, E.F. and Sheffield, J.: Land information system: An interoperable framework for high resolution land surface modeling, Environ. Modell. Softw., 21(10), 1402-1415, https://doi.org/https://doi.org/10.1016/j.envsoft.2005.07.004, 2006.

Li, J., Miao, C.Y., Zhang, G., Fang, Y.H., Wei, S.G. and Niu, G.Y.: Global Evaluation of the Noah-MP Land Surface Model and Suggestions for Selecting Parameterization Schemes, J. Geophys. Res.-Atmos., 127(5), https://doi.org/10.1029/2021JD035753, 2022.

Liang, X., Lettenmaier, D.P., Wood, E.F. and Burges, S.J.: A simple hydrologically based model of land surface water and energy fluxes for general circulation models, Journal of Geophysical Research: Atmospheres, 99(D7), 1994.

Formatted: Indent: Left: 0 cm, Hanging: 2.02 ch, First line: -2.02 ch

Formatted: Font: 10 pt, Font color: Black

Lin, P., Yang, Z., Gochis, D.J., Yu, W., Maidment, D.R., Somos-Valenzuela, M.A. and David, C.H.: Implementation of a vector-based river network routing scheme in the community WRF-Hydro modeling framework for flood discharge simulation, Environ. Modell. Softw., 107, 1-11, https://doi.org/10.1016/j.envsoft.2018.05.018, 2018.

Liu, Y.: Source code for NMH-CS 1.0, Science Data Bank, https://doi.org/10.57760/sciencedb.16102, 2024a.

Liu, Y.: A 3-hourly meteorological forcing dataset for land surface modeling for the Yellow River Basin and North China, Science Data Bank, https://doi.org/10.57760/sciencedb.13122, 2024b.

Liu, Y., Yang, Z. and Lin, P.: Parallel river channel routing computation based on a straightforward domain decomposition of river networks, J. Hydrol., 625, https://doi.org/10.1016/j.jhydrol.2023.129988, 2023.

Ma, N., Niu, G., Xia, Y., Cai, X., Zhang, Y., Ma, Y. and Fang, Y.: A Systematic Evaluation of Noah-MP in Simulating Land-Atmosphere Energy, Water, and Carbon Exchanges Over the Continental United States, J. Geophys. Res.-Atmos., 122(22), 12245-12268, https://doi.org/10.1002/2017JD027597, 2017.

Niu, G., Yang, Z., Mitchell, K.E., Chen, F., Ek, M.B., Barlage, M., Kumar, A., Manning, K., Niyogi, D., Rosero, E., Tewari, M. and Xia, Y.: The community Noah land surface model with multiparameterization options (Noah-MP): 1. Model description and evaluation with local-scale measurements, J. Geophys. Res.-Atmos., 116(D12109), https://doi.org/10.1029/2010JD015139, 2011.

Rodell, M., Houser, P.R., Jambor, U., Gottschalck, J. and Mitchell, K.: The global land data assimilation system, B. Am. Meteorol. Soc., 85(3), 381-394, 2004.

Taylor, K.E.: Summarizing multiple aspects of model performance in a single diagram, Journal of Geophysical Research: Atmospheres, 106(D7), 7183-7192, https://doi.org/https://doi.org/10.1029/2000JD900719, 2001.

Wu, W., Yang, Z. and Barlage, M.: The Impact of Noah-MP Physical Parameterizations on Modeling Water Availability during Droughts in the Texas-Gulf Region, J. Hydrometeorol., 22(5), 1221-1233, https://doi.org/10.1175/JHM-D-20-0189.1, 2021.

Yang, Q., Dan, L., Lv, M., Wu, J., Li, W. and Dong, W.: Quantitative assessment of the parameterization sensitivity of the Noah-MP land surface model with dynamic vegetation using ChinaFLUX data, Agr. Forest Meteorol., 307, https://doi.org/10.1016/j.agrformet.2021.108542, 2021.

Yang, Z., Niu, G., Mitchell, K.E., Chen, F., Ek, M.B., Barlage, M., Longuevergne, L., Manning, K., Niyogi, D., Tewari, M. and Xia, Y.: The community Noah land surface model with multiparameterization options (Noah-MP): 2. Evaluation over global river basins, J. Geophys. Res.-Atmos., 116(D12110), https://doi.org/10.1029/2010JD015140, 2011.

Zheng, H., Yang, Z.L., Lin, P.R., Wei, J.F., Wu, W.Y., Li, L.C., Zhao, L. and Wang, S.: On the Sensitivity of the Precipitation Partitioning Into Evapotranspiration and Runoff in Land Surface Parameterizations, Water Resour. Res., 55(1), 95-111, https://doi.org/10.1029/2017WR022236, 2019.

~~References~~

~~Bales, J., 2019. Featured Collection Introduction: National Water Model II. J. Am. Water Resour. As., 55(4): 938-939, https://doi.org/10.1111/1752-1688.12786.~~

~~Chang, M. et al., 2020. An optimal ensemble of the Noah-MP land surface model for simulating surface~~

heat fluxes over a typical subtropical forest in South China. Agr. Forest Meteorol., 281, https://doi.org/10.1016/j.agrformet.2019.107815.

Chen, F. et al., 2007. Description and evaluation of the characteristics of the NCAR high-resolution land data assimilation system. J. Appl Meteorol Clim, 46(6): 694-713, https://doi.org/10.1175/JAM2463.1.

Francesca, V. et al., 2020. A Multiscale, Hydrometeorological Forecast Evaluation of National Water Model Forecasts of the May 2018 Ellicott City, Maryland, Flood. J. Hydrometeorol., 21(3).

Gan, Y. et al., 2019. Assessment and Reduction of the Physical Parameterization Uncertainty for Noah-MP Land Surface Model. Water Resour. Res., 55(7): 5518-5538, https://doi.org/10.1029/2019WR024814.

Gao, Y., Li, K., Chen, F., Jiang, Y. and Lu, C., 2015. Assessing and improving Noah-MP land model simulations for the central Tibetan Plateau. J. Geophys. Res.-Atmos., 120(18): 9258-9278, https://doi.org/10.1002/2015JD023404.

Gochis, D.J.A.C., 2020. The WRF-Hydro modeling system technical description (version 5.1.1). NCAR Tech. Note.

He, C. et al., 2023. Modernizing the open-source community Noah with multi-parameterization options (Noah-MP) land surface model (version 5.0) with enhanced modularity, interoperability, and applicability. Geosci Model Dev, 16(17): 5131-5151, https://doi.org/10.5194/gmd-16-5131-2023.

Karki, R., Krienert, J.M., Hong, M. and Steward, D.R., 2021. Evaluating Baseflow Simulation in the National Water Model: A Case Study in the Northern High Plains Region, USA. J. Am. Water Resour. As., 57(2): 267-280, https://doi.org/10.1111/1752-1688.12911.

Li, J. et al., 2022. Global Evaluation of the Noah-MP Land Surface Model and Suggestions for Selecting Parameterization Schemes. J. Geophys. Res.-Atmos., 127(5), https://doi.org/10.1029/2021JD035753.

Liang, X., Lettenmaier, D.P., Wood, E.F. and Burges, S.J., 1994. A simple hydrologically based model of land surface water and energy fluxes for general circulation models. Journal of Geophysical Research: Atmospheres, 99(D7).

Lin, P. et al., 2018. Implementation of a vector-based river network routing scheme in the community WRF-Hydro modeling framework for flood discharge simulation. Environ. Modell. Softw., 107: 1-11, https://doi.org/10.1016/j.envsoft.2018.05.018.

Liu, Y., Yang, Z. and Lin, P., 2023. Parallel river channel routing computation based on a straightforward domain decomposition of river networks. J. Hydrol., 625, https://doi.org/10.1016/j.jhydrol.2023.129988.

Ma, N. et al., 2017. A Systematic Evaluation of Noah-MP in Simulating Land-Atmosphere Energy, Water, and Carbon Exchanges Over the Continental United States. J. Geophys. Res.-Atmos., 122(22): 12245-12268, https://doi.org/10.1002/2017JD027597.

Niu, G. et al., 2011. The community Noah land surface model with multiparameterization options (Noah-MP): 1. Model description and evaluation with local-scale measurements. J. Geophys. Res.-Atmos., 116(D12109), https://doi.org/10.1029/2010JD015139.

Rodell, M., Houser, P.R., Jambor, U., Gottschalck, J. and Mitchell, K., 2004. The global land data assimilation system. B. Am. Meteorol. Soc., 85(3): 381-394.

Taylor, K.E., 2001. Summarizing multiple aspects of model performance in a single diagram. Journal of Geophysical Research: Atmospheres, 106(D7): 7183-7192, https://doi.org/https://doi.org/10.1029/2000JD900719.

Wu, W., Yang, Z. and Barlage, M., 2021. The Impact of Noah-MP Physical Parameterizations on

Modeling Water Availability during Droughts in the Texas-Gulf Region. J. Hydrometeorol., 22(5): 1221-1233, https://doi.org/10.1175/JHM-D-20-0189.1.

Yang, Q. et al., 2021. Quantitative assessment of the parameterization sensitivity of the Noah-MP land surface model with dynamic vegetation using ChinaFLUX data. Agr. Forest Meteorol., 307, https://doi.org/10.1016/j.agrformet.2021.108542.

Yang, Z. et al., 2011. The community Noah land surface model with multiparameterization options (Noah-MP): 2. Evaluation over global river basins. J. Geophys. Res. Atmos., 116(D12110), https://doi.org/10.1029/2010JD015140.

Yonghe Liu, 2024a. A 3-hourly meteorological forcing dataset for land surface modeling for the Yellow River Basin and North China. V1. Science Data Bank, https://doi.org/10.57760/sciencedb.13122.

Yonghe Liu., 2024b. Source code for NMP-Hydro 1.0. V1. Science Data Bank, https://doi.org/10.57760/sciencedb.16102.

Zheng, H. et al., 2019. On the Sensitivity of the Precipitation Partitioning Into Evapotranspiration and Runoff in Land Surface Parameterizations. Water Resour. Res., 55(1): 95-111, https://doi.org/10.1029/2017WR022236.

Page 6: [1] Formatted	sucksis@163.com	2025/1/27 16:44:00

Font: 10 pt, Font color: Auto

Page 6: [1] Formatted	sucksis@163.com	2025/1/27 16:44:00

Font: 10 pt, Font color: Auto

Page 6: [1] Formatted	sucksis@163.com	2025/1/27 16:44:00

Font: 10 pt, Font color: Auto

Page 6: [1] Formatted	sucksis@163.com	2025/1/27 16:44:00

Font: 10 pt, Font color: Auto

Page 6: [1] Formatted	sucksis@163.com	2025/1/27 16:44:00

Font: 10 pt, Font color: Auto

Page 6: [1] Formatted	sucksis@163.com	2025/1/27 16:44:00

Font: 10 pt, Font color: Auto

Page 6: [1] Formatted	sucksis@163.com	2025/1/27 16:44:00

Font: 10 pt, Font color: Auto

Page 6: [2] Formatted	sucksis@163.com	2025/1/27 16:44:00

Font: 10 pt, Font color: Auto

Page 6: [2] Formatted	sucksis@163.com	2025/1/27 16:44:00

Font: 10 pt, Font color: Auto

Page 6: [2] Formatted	sucksis@163.com	2025/1/27 16:44:00

Font: 10 pt, Font color: Auto

Page 6: [2] Formatted	sucksis@163.com	2025/1/27 16:44:00

Font: 10 pt, Font color: Auto

Page 6: [2] Formatted	sucksis@163.com	2025/1/27 16:44:00

Font: 10 pt, Font color: Auto

Page 6: [2] Formatted	sucksis@163.com	2025/1/27 16:44:00

Font: 10 pt, Font color: Auto

Page 6: [3] Formatted	sucksis@163.com	2025/1/27 16:44:00

Font: 10 pt, Font color: Auto

Page 6: [3] Formatted sucksis@163.com 2025/1/27 16:44:00

Font: 10 pt, Font color: Auto

Page 6: [3] Formatted sucksis@163.com 2025/1/27 16:44:00

Font: 10 pt, Font color: Auto

Page 6: [3] Formatted sucksis@163.com 2025/1/27 16:44:00

Font: 10 pt, Font color: Auto

Page 6: [3] Formatted sucksis@163.com 2025/1/27 16:44:00

Font: 10 pt, Font color: Auto

Page 6: [3] Formatted sucksis@163.com 2025/1/27 16:44:00

Font: 10 pt, Font color: Auto

Page 6: [3] Formatted sucksis@163.com 2025/1/27 16:44:00

Font: 10 pt, Font color: Auto

Page 6: [3] Formatted sucksis@163.com 2025/1/27 16:44:00

Font: 10 pt, Font color: Auto

Page 6: [3] Formatted sucksis@163.com 2025/1/27 16:44:00

Font: 10 pt, Font color: Auto

Page 6: [4] Formatted sucksis@163.com 2025/1/27 16:44:00

Font: 10 pt, Font color: Auto

Page 6: [4] Formatted sucksis@163.com 2025/1/27 16:44:00

Font: 10 pt, Font color: Auto

Page 6: [4] Formatted sucksis@163.com 2025/1/27 16:44:00

Font: 10 pt, Font color: Auto

Page 6: [4] Formatted sucksis@163.com 2025/1/27 16:44:00

Font: 10 pt, Font color: Auto

Page 6: [4] Formatted sucksis@163.com 2025/1/27 16:44:00

Font: 10 pt, Font color: Auto

Page 6: [4] Formatted	sucksis@163.com	2025/1/27 16:44:00

Font: 10 pt, Font color: Auto

Page 6: [5] Formatted	sucksis@163.com	2025/1/27 16:44:00

Font: 10 pt, Italic

Page 6: [5] Formatted	sucksis@163.com	2025/1/27 16:44:00

Font: 10 pt, Italic

Page 6: [6] Formatted	sucksis@163.com	2025/1/27 16:44:00

Font: 10 pt

Page 6: [6] Formatted	sucksis@163.com	2025/1/27 16:44:00

Font: 10 pt

Page 6: [6] Formatted	sucksis@163.com	2025/1/27 16:44:00

Font: 10 pt

Page 6: [6] Formatted	sucksis@163.com	2025/1/27 16:44:00

Font: 10 pt

Page 6: [6] Formatted	sucksis@163.com	2025/1/27 16:44:00

Font: 10 pt

Page 6: [6] Formatted	sucksis@163.com	2025/1/27 16:44:00

Font: 10 pt

Page 6: [6] Formatted	sucksis@163.com	2025/1/27 16:44:00

Font: 10 pt

Page 6: [6] Formatted	sucksis@163.com	2025/1/27 16:44:00

Font: 10 pt

Page 6: [6] Formatted	sucksis@163.com	2025/1/27 16:44:00

Font: 10 pt

Page 6: [6] Formatted	sucksis@163.com	2025/1/27 16:44:00

Font: 10 pt

Page 6: [6] Formatted	sucksis@163.com	2025/1/27 16:44:00

Font: 10 pt

Page 6: [6] Formatted	sucksis@163.com	2025/1/27 16:44:00

Font: 10 pt

Page 6: [7] Formatted	sucksis@163.com	2025/1/27 16:45:00

Font: (Default) Times New Roman

Page 6: [7] Formatted	sucksis@163.com	2025/1/27 16:45:00

Font: (Default) Times New Roman

Page 6: [8] Formatted	sucksis@163.com	2025/1/27 16:45:00

Font: 10 pt

Page 6: [8] Formatted	sucksis@163.com	2025/1/27 16:45:00

Font: 10 pt

Page 6: [8] Formatted	sucksis@163.com	2025/1/27 16:45:00

Font: 10 pt

Page 6: [8] Formatted	sucksis@163.com	2025/1/27 16:45:00

Font: 10 pt